SECOND SEMI-ANNUAL REPORT

Nov 30, 1964 to May 31, 1965

under NASA Grant NsG-601

on

"Oscillatory Combustion in Rockets"

Prepared by

R. Sowls

H. Hiroyasu

R. Goluba

D. Wendland

J. Ricart-Lowe

Supervisors

Prof. G.L. Borman

Prof. P.S. Myers

Prof. O.A. Uyehara

Mechanical Engineering Department

University of Wisconsin

Madison, Wisconsin

SECOND SEMI-ANNUAL REPORT TO THE

NATIONAL AERONAUTICS AND SPACE ADMINISTRATION

ON RESEARCH GRANT NsG-601

Nov. 30, 1964 - May 31, 1965

The research being conducted under this grant is aimed at obtaining a more fundamental understanding of some of the aspects of oscillatory combustion. There are three separate, but related, investigations being conducted under this grant. Part A gives a report of research conducted on the measurements of drop size and velocity distributions in sprays. Parts B-1 and B-2 give a report of research conducted on heat transfer from a gas to a solid surface when the gas is undergoing large pressure oscillations. Part C gives a report of research conducted on the vaporization of liquid under conditions where the liquid may pass through its critical point. Some details of the apparatus used in measuring drop sizes and velocities are given in Appendix A.

A. Drop Size Distributions in Sprays

(H. Hiroyasu, R. Sowls)

Over the past several years much work has been done at the University of Wisconsin on developing apparatus and methods for studying droplets in sprays. Prior to the summer of 1964, most of the work done on this project was devoted to developing apparatus and techniques for studying droplets in sprays in which the spray liquid contained a fluorescent dye, and to developing an automatic method of obtaining numerical data from the photographs. At that time, the fluorescent technique was capable of giving spatial drop size distributions at almost any section in the spray. The next step was to try to relate the spatial drop size distributions so obtained to the mass flux.

It is evident that mass flux of a spray liquid is related to drop size by drop velocity. During the past year, the work done on this project has been primarily devoted to extending the fluorescent technique so that it can be used to measure drop velocities in a spray as well as drop sizes. The most obvious method of photographically measuring drop velocities involves focusing a suitable camera so that its depth of focus is parallel to and includes the path of motion of the drop. Then the drop can be illuminated by two very short pulses of light separated by a short known period of time so that two images of each drop will appear on the film. The velocity of the drop can then be calculated from the known camera magnifi-

cation, the known period between the light pulses, and the measured distances between the droplet images on the film. The camera that had been developed previously to obtain drop sizes was thought adequate for drop velocities as well, so the problem was one of obtaining a suitable light source or sources and the related control and measuring devices.

The existing apparatus available to the project one year ago could most easily and most effectively be used if a single, powerful, line light source, capable of being pulsed twice with an accurately controlable period between the pulses of from 10 microseconds to say 100 microseconds were available. Using a single line light source has the advantages of permitting the use of a concave spherical backup mirror for more uniform illumination of the sample space and of requiring only one condensing lens assembly. Because of this, a number of attempts to devise such a light source were made without acceptable results. Next the feasibility of using two separate light sources to act as a single source by superimposing them with various kinds of beam splitters was investigated. Because these methods would throw away at least 50% of the available light, and because the materials necessary to execute these ideas were not readily available, it was decided to modify the existing apparatus to use two separate light sources. This approach was moderately successful. The details of the apparatus as well as some other less successful methods are discussed in Appendix A.

A schematic of part of the apparatus finally developed for taking drop size and velocity data is shown in Fig. 1. This figure does not show the control and monitoring gear. The capability of a second timed light pulse was obtained by replacing a concave mirror that had been on the left (directions will always be specified for an observer looking from behind the camera) in the single flash apparatus by a light source and condensing lens assembly similar to that on the right, and providing the necessary timing and triggering functions. The various elements of the apparatus are described in Appendix A.

Referring to Fig. 1 the apparatus is adjusted as follows. The light sources and condensing lenses on both sides are positioned so that they can illuminate the field of view of the camera. This is a region 0.16 in. high by 0.20 in wide by 200 microns thick and will be called the sample space and the camera object space. Then the nozzle is positioned so that the paths of motion of the drops in the region of the spray being studied lie in this sample space. The spray is directed into a duct and drawn out by an exhaust fan. The room in which the experiment is carried out is darkened since the camera has no shutter, and this prevents fogging of the film between exposures. Pictures are taken with the delay between the two light pulses adjusted to suit the spray operating conditions. Enough timed double exposures are taken on each piece of film to give a reasonable number of images, i.e., enough not to be wasteful but few enough so that data recovery will not be

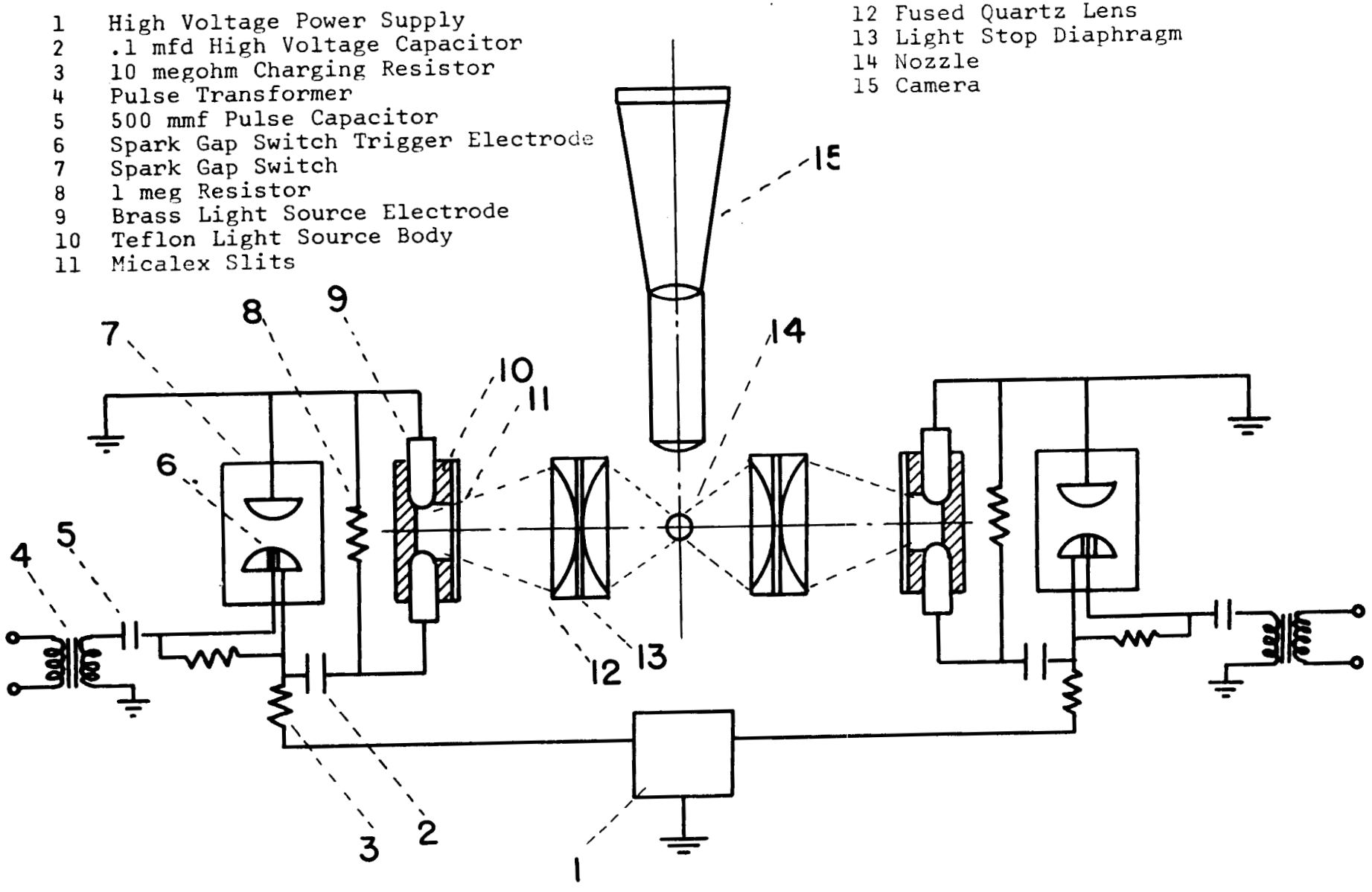

Fig. 1 - Schematic of Part of the Double Flash Apparatus

confused by crowding or overlapping images. Enough pieces of film are used at each spray position and condition to give greater than the minimum number of images that are required for analysis. Because the sample space is so small, the nozzle must be repositioned many times for each section through the spray that is being investigated.

The purpose of presenting the drop photographs in Figs. 2 and 3 is to illustrate the kind of velocity data that can be taken with the fluorescent technique at its present level of development. The photographs are of an ethyl alcohol spray, containing 5 grams per liter of Fluorescein water soluble Uranin dye, formed by Monarch F-80 swirl type nozzle. These photographs are contact prints made from the actual negatives produced by the camera, but are cut down for more compact presentation.

Two flaws that can be noticed from the photographs are that one side of each drop is brighter than the other and that in some cases, there appears to be some motion blur. The bright side of the image arises from the fact that in the present setup, the drops are illuminated from only one side at a time. This could be corrected if a concave mirror could be incorporated opposite each light source to focus the diverging light sheet back onto the sample space. This could most easily be done if a single line light source could be used for both light pulses. The motion blur arises from the finite duration of the light pulses (about 2 microseconds). For a 10 meter per second droplet velocity, a 2 microsecond light

pulse duration produces a motion blur of 0.5 mm on the film. If the leading edges of the images were sharp enough, accurate velocity measurements could be made even with motion blur. When the image on the film is magnified 4 or 5 times, however, it becomes difficult to decide where the leading edges of the drops are and measurements of high precision cannot be made. This fault can only be corrected if sufficiently powerful light sources of extremely short duration and whose output wavelengths efficiently excite the fluorescent dye can be obtained.

The pictures shown in Fig. 2 were all taken with the left edge of the film along the spray axis with a pressure drop across the nozzle of 40 psi, and a delay of 10 microseconds between light pulses. The distance of the sample space downstream of the nozzle tip and the number of timed delay double exposures represented are given in the heading below each picture.

Some observations that can be made from the photographs of Fig. 2 are:

1. Close to the nozzle (Fig. 2a) there is a little break-up into droplets but the majority of the liquid is flowing as a sheet or film.

2. Farther from the nozzle (Fig. 2b) breakup of the liquid into droplets is nearly completed but many of the droplets are irregularly shaped.

3. Still farther from the nozzle (Fig. 2c and Fig. 2d) the droplets all have circular profiles.

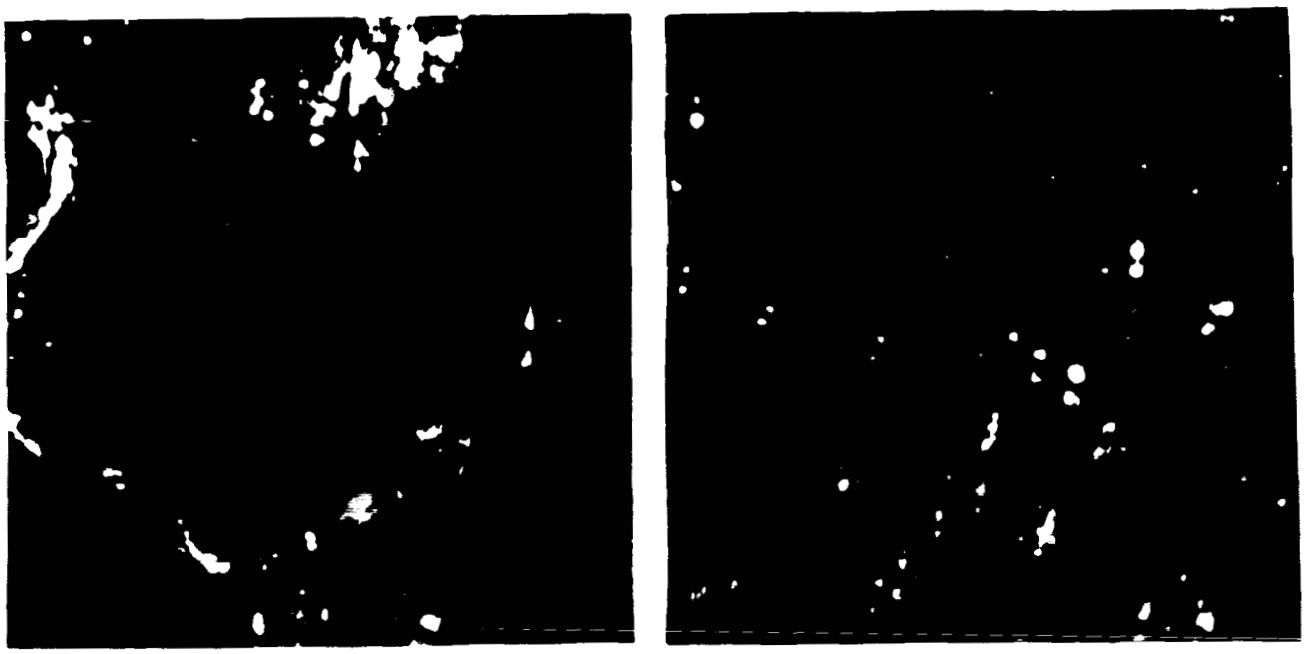

a) D = 0.20 in. = 1 [illegible]

b) D = 0.35 in. [illegible]

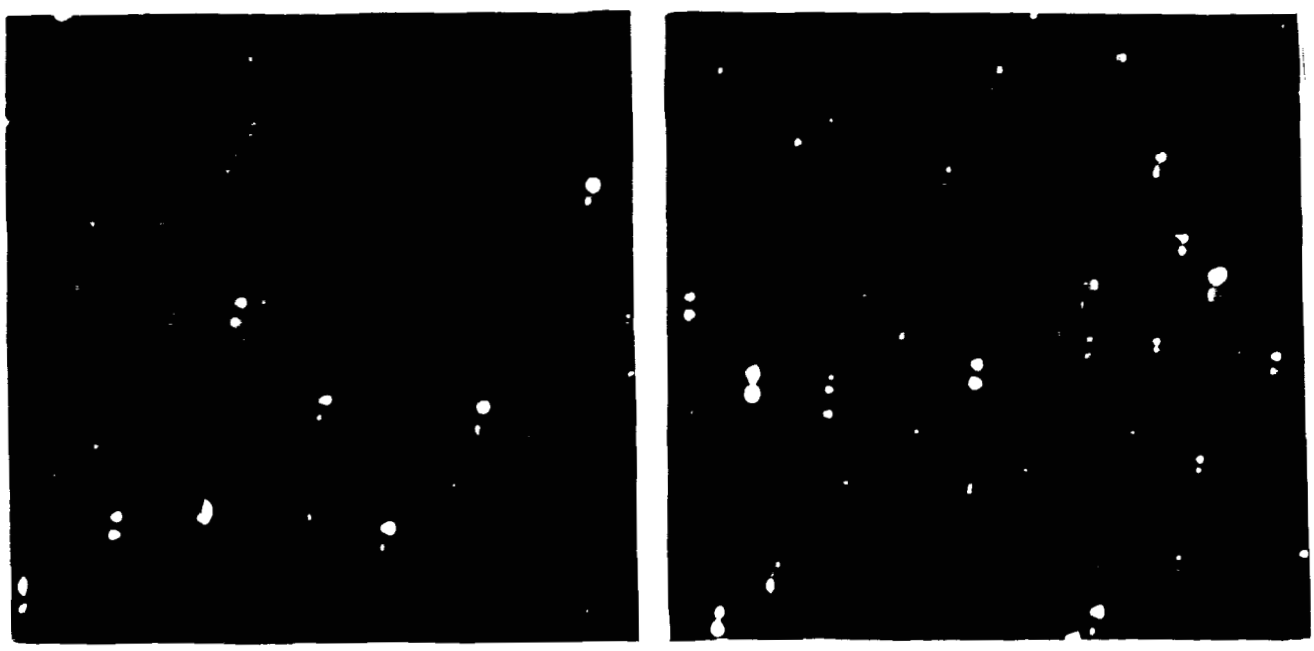

c) D = 1.30 in., E = 4

d) D = 2.30 [illegible]

Fig. 2. Photographic [illegible] of various positions along [illegible] axis with 40 psi [illegible] pressure and 10 psec [illegible] light pulses. D is [illegible] from the nozzle [illegible] number of timed double exposures represented by each [illegible]

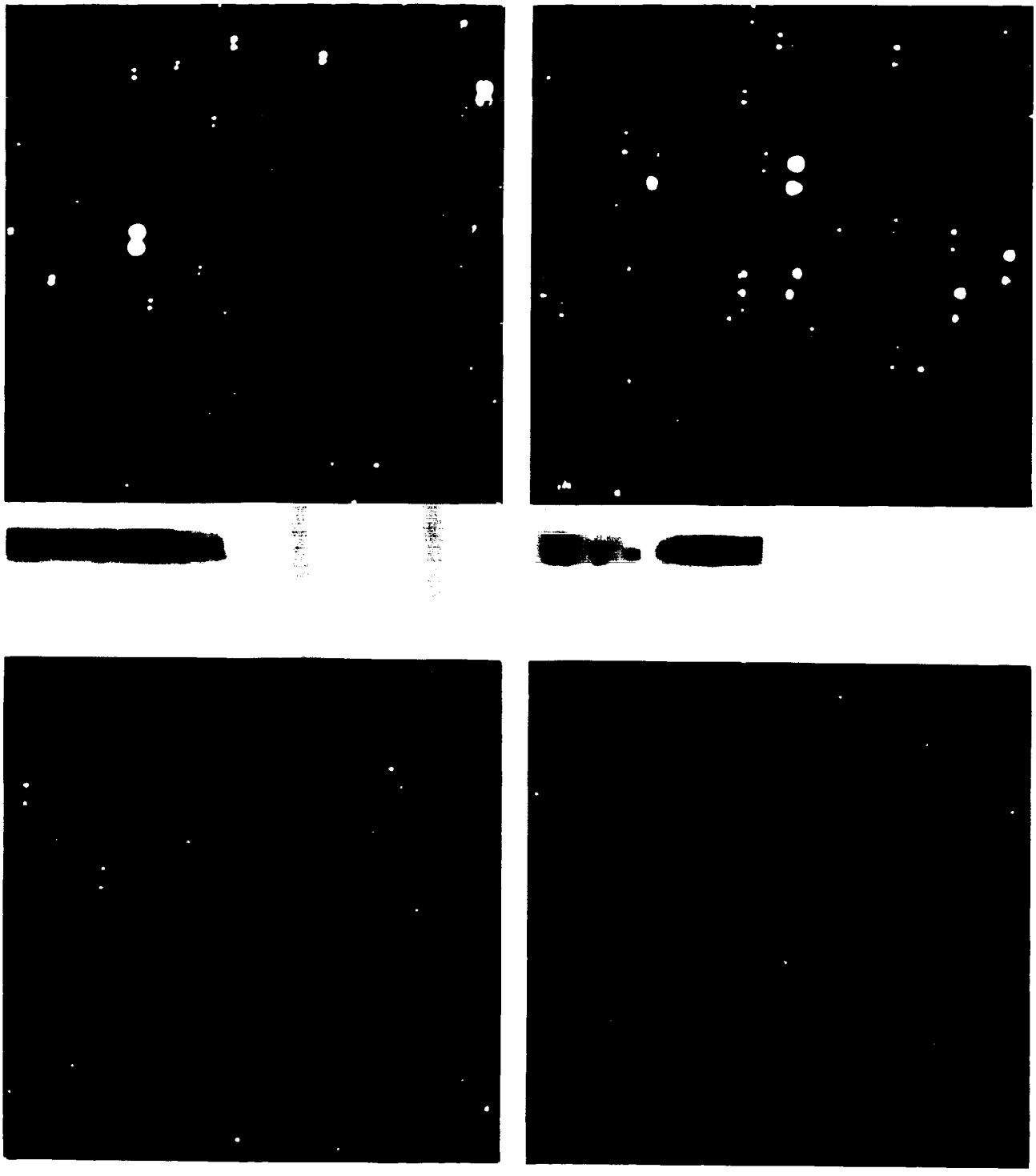

c) P = 60 psi

d) P = 80 psi

Fig. 3. Photographs taken of a position 2.30 in. downstream and just to the left of the spray axis for injection pressures as marked. Five timed double exposures with a delay of [illegible] between light [illegible] are represented in each photograph.

4. The separation between image pairs decreases going downstream indicating that the droplets are slowing down toward the air velocity.

5. The average droplet diameter appears to be about the same in Fig. 2c and Fig. 2d which should be true in a steady flow case with negligible vaporization and no breakup between sections.

The photographs presented as Fig. 3 were all taken with the left edge of the sample space along the spray axis and with its lower edge 2.30 inches from the nozzle tip. Five double exposures with a delay of 15 microseconds between the light pulses are represented on each film. Pressure drops across the nozzle of 20, 40, 60, and 80 psi are represented as marked under each photograph.

The most noticable thing about these pictures is that the average drop diameter decreases with increased injection pressure while the velocity of drops of comparable size increases with increased pressure. No attempt is made here to relate the observations to each other and to the operating conditions. Mr. John Groeneweg who is now at NASA Lewis Laboratories is currently analyzing these data as part of his Ph.D. thesis.

B-1. Heat Transfer with Pressure Pulsations in a Non-Flow System

(D. Wendland)

The purpose of the project is to study unsteady heat transfer to a metal surface from a gas undergoing intermediate frequency pressure and temperature oscillations in a non-flow system. The periodic pressure and temperature pulsations are generated by a high speed chain saw crankcase, piston, and cylinder. The technique is to measure instantaneous pressure, head gas-side surface temperature, and the gas temperature at several locations in the gas near the head surface. Wall heat transfer is calculated from the wall temperature history with the aid of infinite plate theory. Pressure is indicated by a Li-Draper transducer; surface temperature is measured by a surface thermocouple with .00004 in. junction thickness; gas temperature is monitored with resistance thermometers of very small time constant.

The crankcase, piston, and cylinder originally used in this investigation proved to be inadequate for a number of reasons. Principal difficulties were experienced with deterioration of the gas temperature measuring instrumentation; these resistance wires are constructed of .0001 inch platinum and platinum - 10% Rhodium wires, and the presence of oil droplets passed by the piston rings, coupled with the turbulence and vibration levels of the system, limited the effective instrument life to less than a minute.

A small, high-speed crankcase requiring no crankcase oil supply was installed and fitted with teflon-based piston rings to do away with cylinder-wall lubrication. Difficulty has been experienced with piston scuffing limiting ring life to 30 minutes or so, but it is anticipated this time can be increased or tolerated if necessary. Resistance wires have remained intact for at least 20 minutes. The mean cylinder pressure level is controlled by a pressurized system connected to a set of holes in the cylinder wall near the bottom dead center of piston travel.

Calibration of the temperature and pressure signals is effected with a combination of simple circuitry and an assembly of eight adjustable cam-breaker point sets which was constructed and installed.

The bridges used in conjunction with the resistance wires were constructed and calibrated, producing .072 mv/°F when used with Pt - 10% Rh wires. Five transistorized amplifiers were obtained, calibrated for phase shifting, and mounted; they are Astrodata model 885 wideband differential DC amplifiers, with variable gain to 3000.

Fig. 4 shows a pressure-time trace. Relevant data are:

frequency: 15.4 cps (920 rpm)

pressure ratio: $\frac{P_{max}}{P_{min}}$ 18.4 (8.25 comp. ratio, P_{max}=263 psi, P_{min}=14.3 psi)

computed bulk temp. ratio:

$\frac{T_{max}}{T_{min}}$ 2.23 (T_{max} = 770 °F

T_{min} = 92 °F)

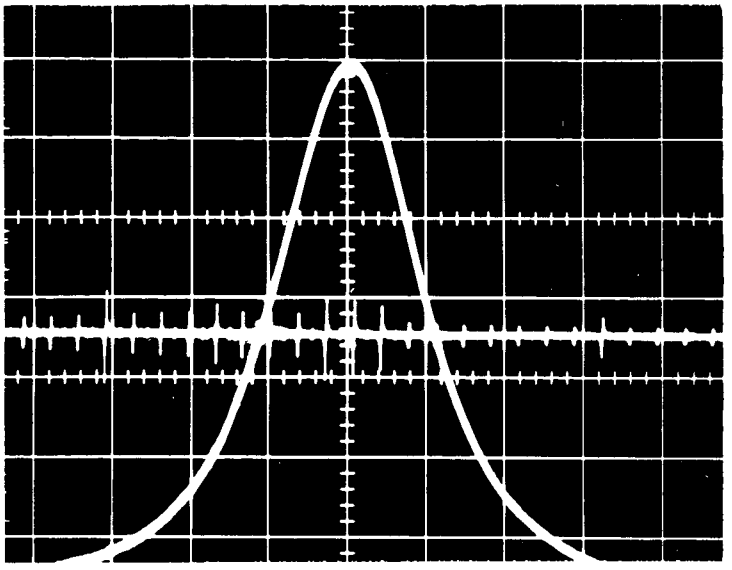

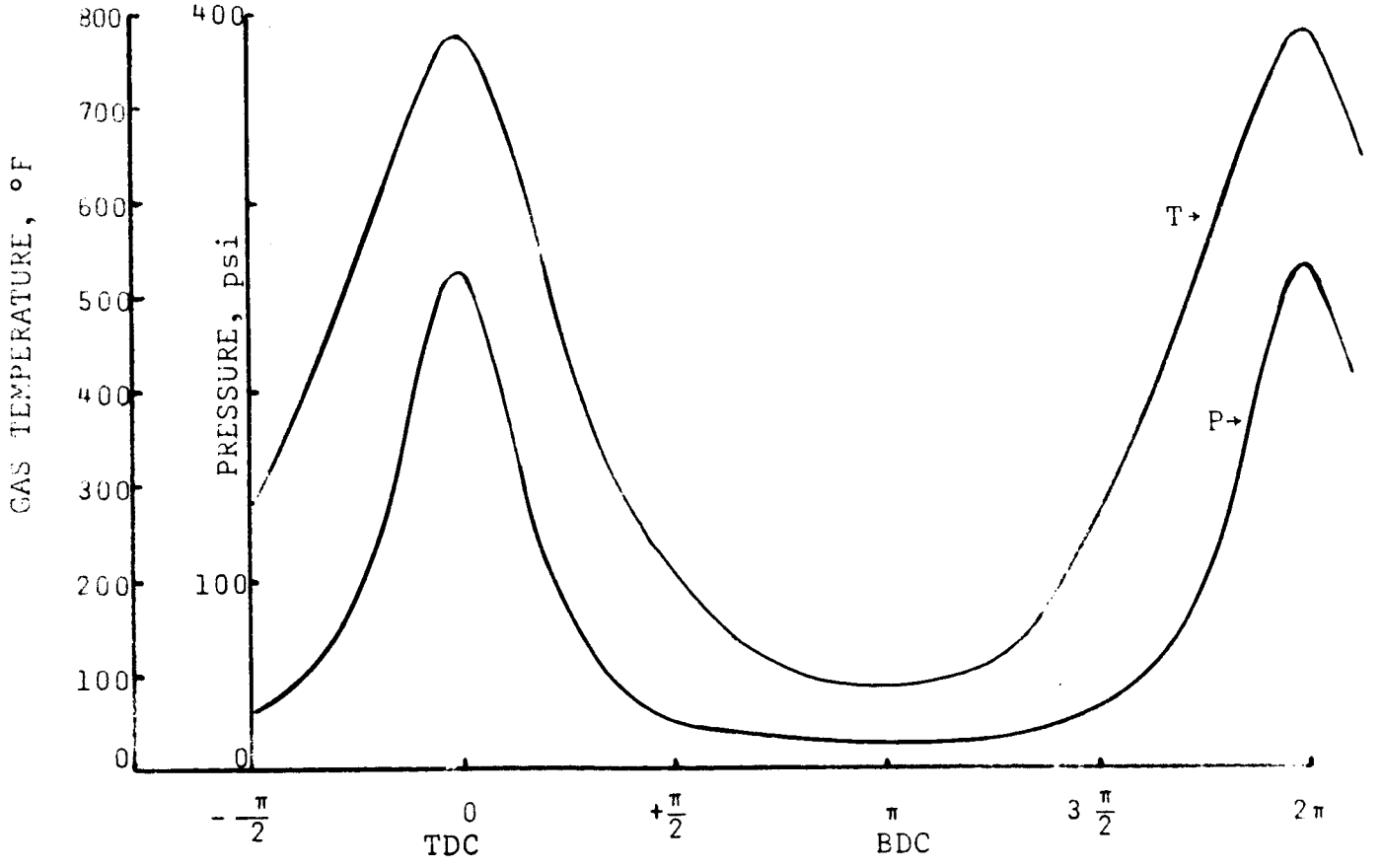

Fig. 4 - Pressure and Temperature as a Function of Piston Position

measured pressure peak occurs at about	1° BTC
computed bulk temperature peak occurs at about	3° BTC
pressure-volume relationship very close to polytropic at a non-measurable index	

The principal instrumentation effort was and is being applied to the gas temperature measuring resistance wires with a time constant near .2 millisec. The wires are typically of Pt - 10% Rh, .0001 inch diameter, 1/4" to 1/2" long, and mounted to constantan leads with conductive silver epoxy. They are etched to this size in a nitric acid solution. Aside from the mechanical strength difficulties, a certain amount of electrical instability were noted and ascribed to fluctuations in the contact resistance in the silver epoxy between the wires and leads. Copper leads were tried with no improvement. Apparently, the epoxy ages upon being exposed to compression temperatures, and the contact resistance, often several times the actual wire resistance with which it is in series, changes and throws the bridge into unpredictable imbalance. Unsuccessful attempts were made to "heat soak" the instrument to stabilize it. Cold soldering was tried as a replacement mounting technique, but the interaction of soldering flux and nitric acid in the etching process which occurs after mounting repeatedly destroyed the wires. Silver soldering is very difficult due to the presence of a 4000 °F flame near the fragile wires, but it is being attempted.

Another tack to the problem of measuring gas temperature is to use relatively large (.0004 inch) quartz fibers with a baked-on platinum shell as the measuring instrument. A time constant less than 10 microseconds is anticipated. The fibers have a starch-oil (organic) coating applied in the early stages of manufacture; this coating must be removed prior to the platinum deposition by heating to 500 °F. The platinum is applied in the form of an organic Au - Pt mixture which bakes to a .000005 inch platinum coating at 1022 °F. Mounting of the quartz fibers is being tried by silver soldering with a miniature butane-oxygen torch.

B-2. The Effect on Heat Transfer of Large Amplitude Pressure Oscillations in a Flowing Fluid

(R. Goluba)

In the past six months, much of the effort has been directed at preliminary design of the apparatus and the acquisition of the associated equipment. A schematic diagram of the research apparatus is shown in Fig. 5. Large amplitude pressure oscillations are produced in a pipe (station G to station H) by periodically interrupting the flow by use of a rotating siren disk located upstream from the test section. Air is supplied from ten high-pressure (2200 psia) air cylinders. A constant mass flow rate during a run can be maintained by the use of an automatic control valve located at the outlet of the bank of air cylinders. A high pressure air compressor will then be used to refill the air cylinders after each run.

A computer program was available to determine the magnitude of the pressure oscillations in the pipe as well as the shape of the pressure oscillations that could be obtained from this apparatus. The computer program was not run long enough for steady state conditions to be achieved in the tube since this would have resulted in the use of an excessive amount of computer time. The computer time required is large because the high frequency of the oscillations (500 cps) requires that small time increments be used in the program. Typical profiles of the pressure waves obtained from the computer program are shown in Figs. 6 and 7. The pressure wave at the midpoint of

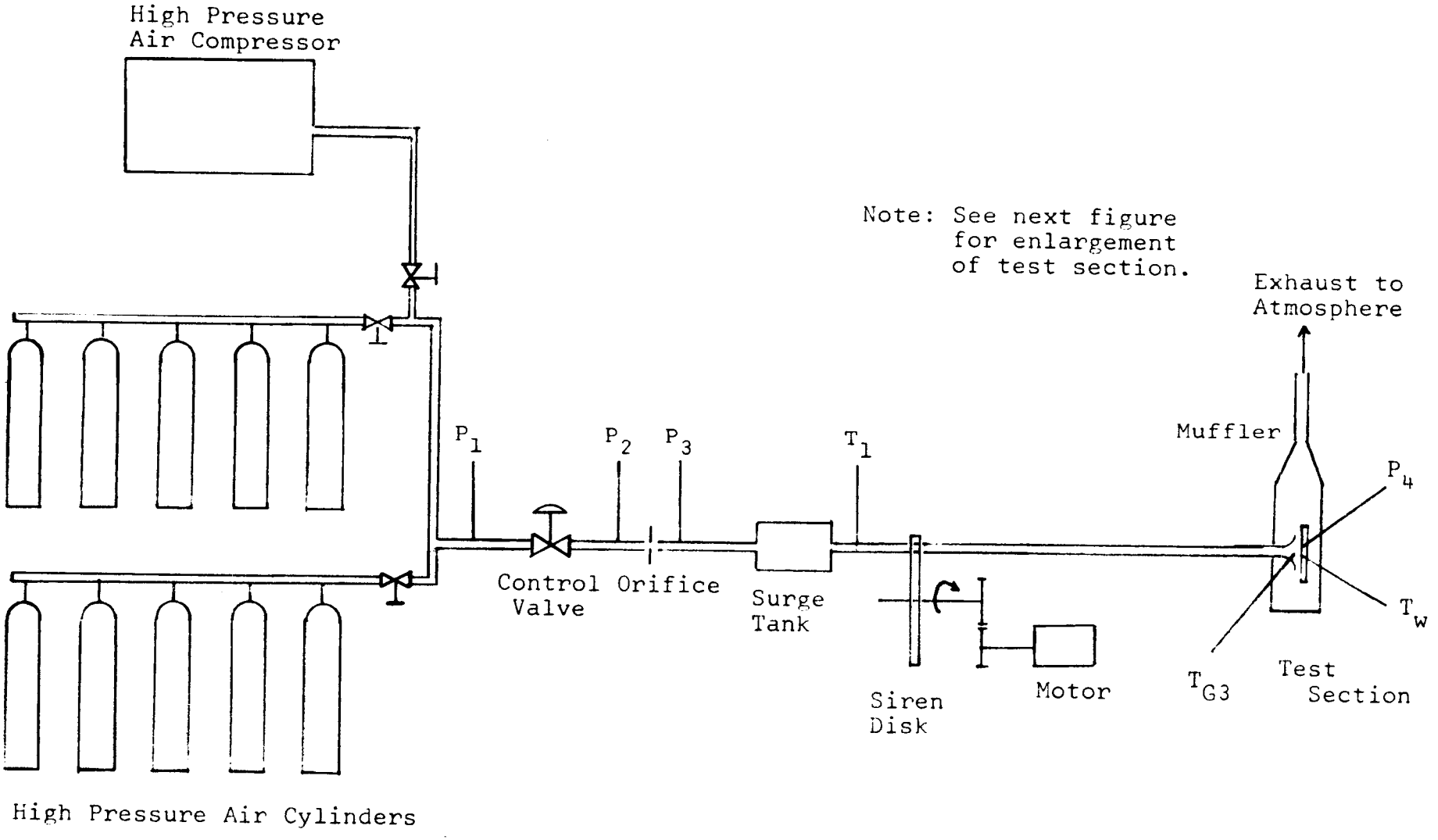

Fig. 5 - Schematic of Apparatus for Pulsating Flow

the pipe (Fig. 6) is quite similar to the shock-type pressure waves produced in a rocket chamber experiencing unstable combustion -- a steep rise in pressure followed by a gradual decrease. As expected, this was the same type of pressure wave which has been obtained in a similar apparatus at Princeton University. At the outlet of the pipe the magnitude of the pressure oscillation as well as the steepness of the pressure front is decreased since the presence of the outlet tends to dampen the oscillations somewhat.

An enlargement of the test section is given in Fig. 8. The effect of the pressure oscillations on the heat transfer to a flat plate normal to the flow is to be investigated. The gas temperature, T_{G3}, will oscillate in a manner similar to the pressure due to the compression of the gas. This gas temperature fluctuation causes the surface temperature, T_w, of the flat plate to fluctuate about some mean value.

To better understand the mechanism by which the heat transfer is increased by the presence of pressure oscillations, it is desirable to determine the instantaneous variation of the surface temperature and the heat flux. However, this is a rather formidable task due to the magnitude of the surface temperature fluctuations. An order of magnitude estimate of the surface temperature fluctuation can be obtained by utilizing the solution given by Carslaw and Jaeger in Conduction of Heat in Solids, page 74, for the case of a constant heat transfer coefficient and a sinusoidal gas temperature variation. It should

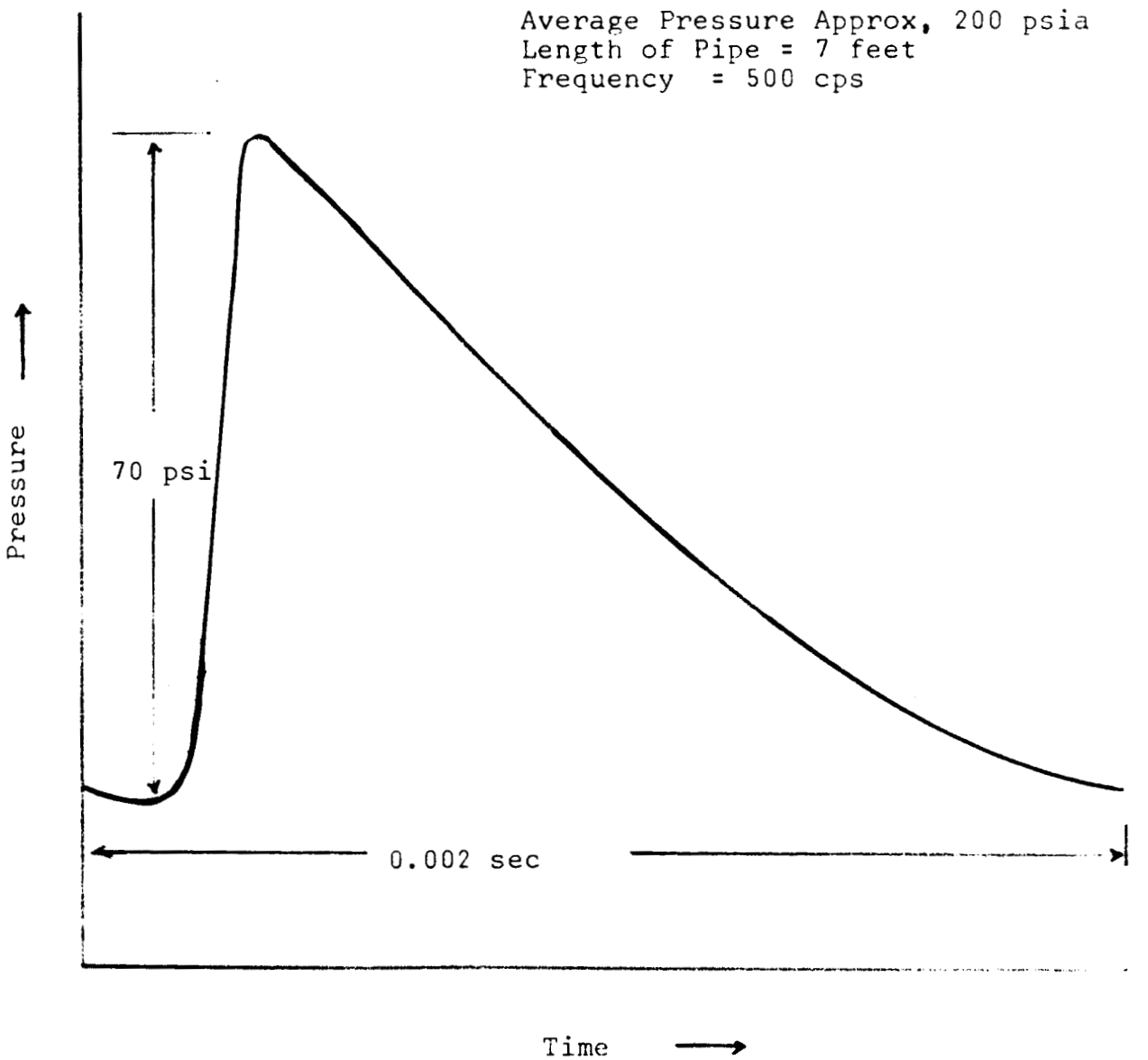

Fig. 6 - Typical Computed Pressure Wave at Midpoint of Pipe

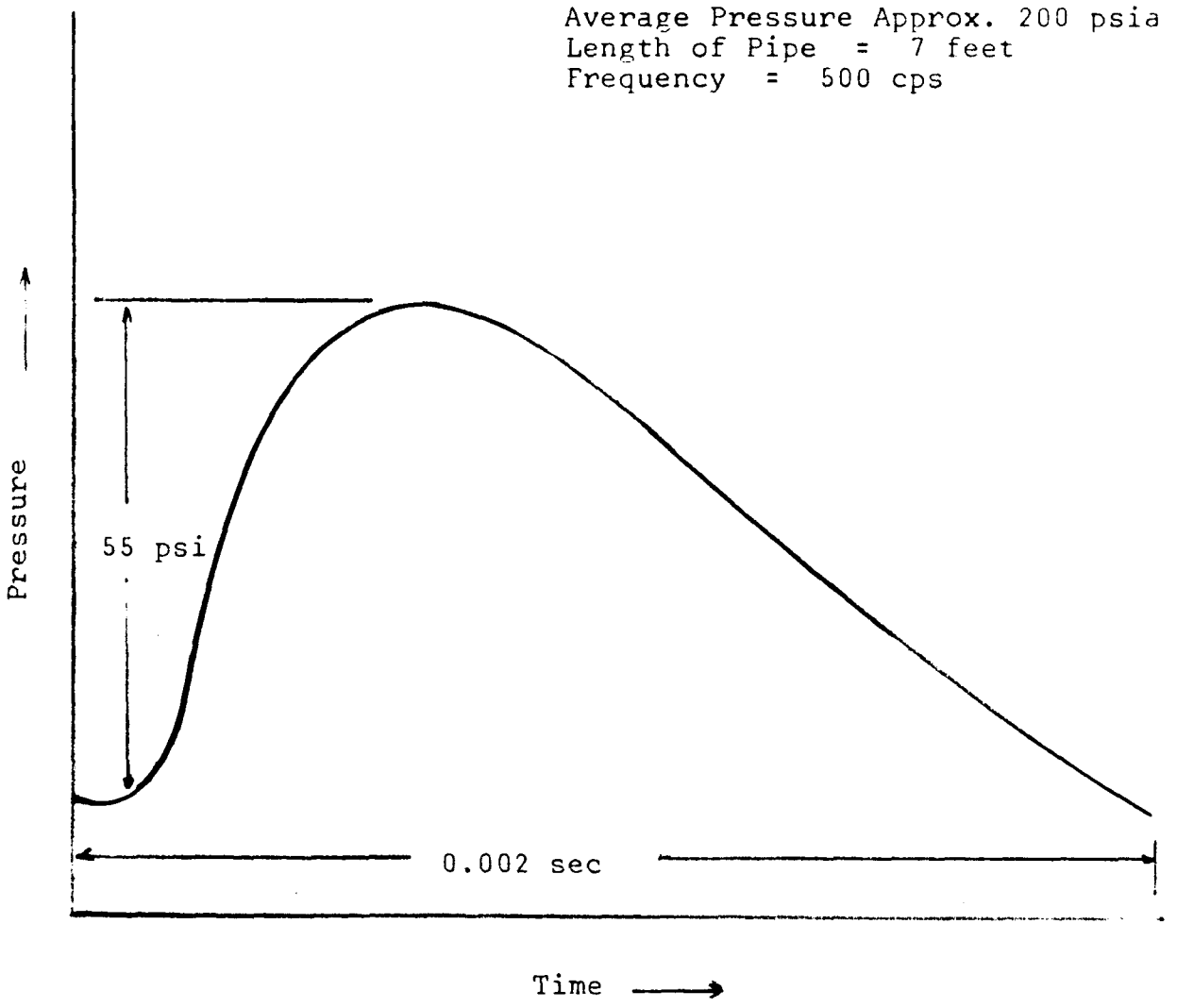

Fig. 7 - Typical Computed Pressure Wave at Outlet of Pipe

be emphasized that this is only an estimate since the heat transfer coefficient probably varies with time and, in fact, one is not sure if the concept of a heat transfer coefficient should be used in the case under investigation. For a variation in gas temperature of 30 °F at 500 cps, which would correspond to a 50 psi pressure fluctuation about a mean of 200 psia, the amplitude of the surface temperature fluctuation is less than $\pm$ .025 °F when the plate material is steel. Even though the surface temperature fluctuations are small, the fluctuations in heat flux at the surface are large -- $\pm$ 6000 BTU/hr-ft^2. Although the variation in heat flux is large, only small energy fluctuations occur at the rather large frequencies of interest (500 - 1000 cps). Of course, this is reflected in that the surface temperature fluctuation, as well as the penetration depth of the temperature fluctuations into the plate, is small. A thin film thermocouple will be used to measure the surface temperature. The temperature fluctuations are so small that it becomes necessary to measure voltage fluctuations as small as several microvolts. This requires an extremely noise free amplifier so that a usable trace can be displayed on an oscilloscope. If the measurement problems become insurmountable, one can gain a 20 fold increase in the surface temperature fluctuation by changing the surface material from steel to bakelite. In fact, it is desirable to investigate the heat transfer to a material such as bakelite since the physical properties of bakelite are similar to those of a fuel such as

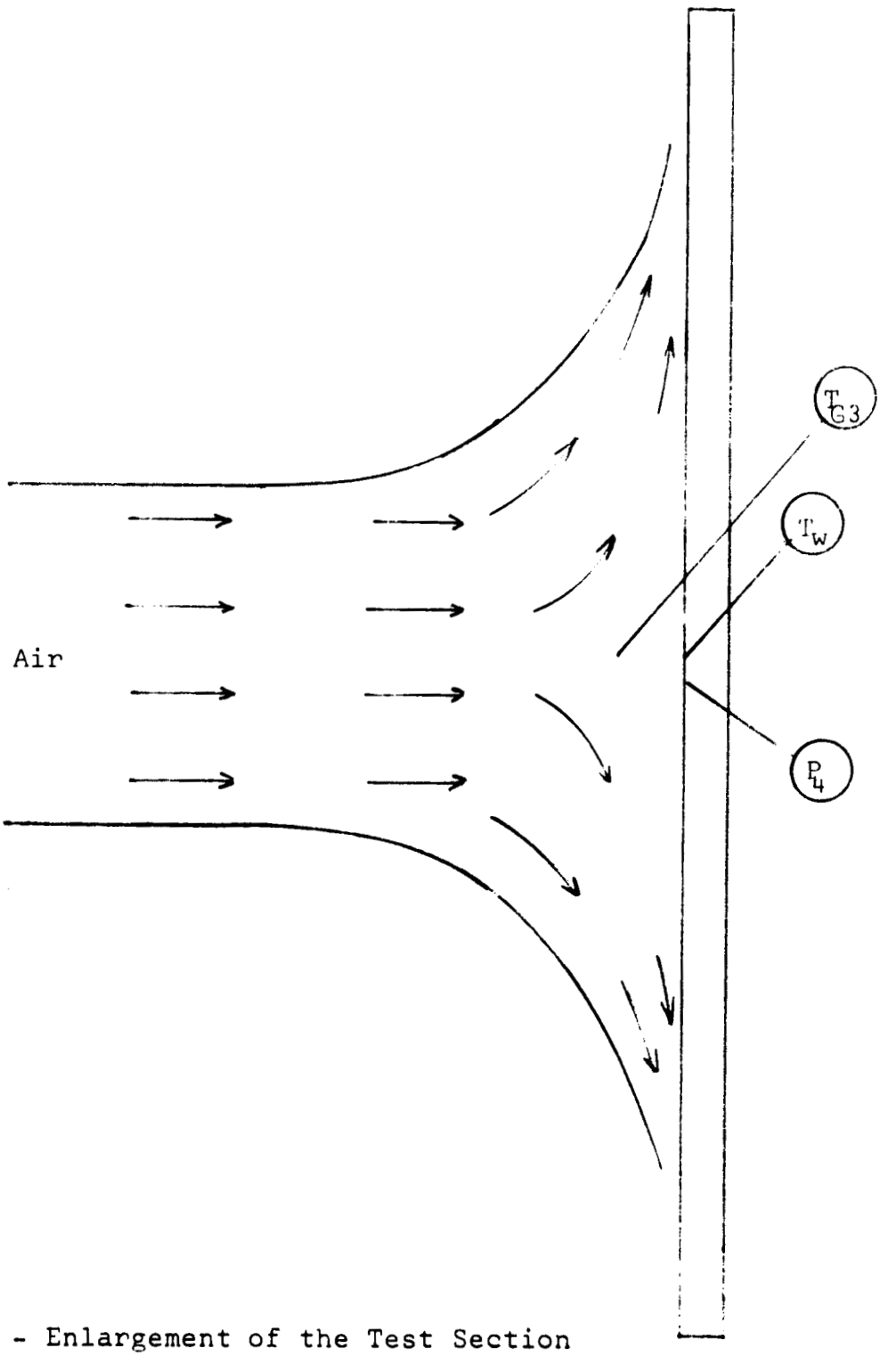

Fig. 8 - Enlargement of the Test Section

kerosene. Information regarding the phase relationship between the gas temperature and surface temperature of a material with properties similar to a fuel would be helpful in understanding the energy exchanges which occur during unstable combustion.

C. Vaporization in the Region of the Critical Point

As previously reported the first six months were spent primarily in acquainting the students with the problem, setting up some computer programs, and investigating various experimental procedures.

After investigation of a number of experimental procedures, it was decided that the first experiments should be restricted to studying steady-state phenomena but to maintain the basic droplet geometry. Apparatus is now being constructed which will use a droplet hanging from a probe and being continuously fed with fresh liquid. The droplet size will be observed optically. By control of the liquid feed rate, it should be possible to obtain a non-changing droplet diameter. The liquid temperature will be measured by thermocouples in the drop and immediately before the liquid flows into the drop. The temperature of the liquid being added to the drop can thus be adjusted to be the same as the measured droplet core temperature. Under these adjusted conditions, steady-state vaporization should prevail. The measured quantities would be air temperature and velocity, droplet diameter, vaporization rate, and droplet core temperature. As a first step in designing the set-up, a suitable liquid had to be chosen. The desired characteristics were

a. low critical temperature,

b. moderate critical pressure (below 1000 psi),

c. relatively high surface tension,

d. well studied substance so that physical properties could be obtained from the literature,

e. liquid of interest in rocket combustion.

A preliminary review of critical constants yielded several possible choices: the lower hydrocarbons, some Freons, and some alcohols. After further examination, it was decided to investigate Freon-13 further. This compound satisfied the first two requirements. It, however, does not have a large surface tension. Its thermodynamic properties have been fairly well studied, but little is known about its transport properties. It is not a propellant and its chemical structure is complex.

Despite the many objections to Freon-13, it was chosen because of its low critical temperature, 82.5 °F. Calculations were performed for the steady state temperature. Fig. 9 shows the resulting curve for a pressure of 600 psia (1.07 P_c). Upon analysis of the results, several interesting characteristics of the property equations used in these calculations were observed. The Schmidt number which for most substances is approximately unity, was nearly eight at the critical point. The ratio of the thermal Nusselt number to the mass Nusselt number was calculated to be approximately two. Here again, for most known substances this ratio is approximately one. Since it was uncertain whether these results were caused by the unusual behavior of Freon-13 or by poor estimates of the properties, it was decided to try to check the transport properties of Freon by comparing them with the transport properties of a better known substance. This was done by taking n-dodecane and calculating its diffusivity coefficient by two different methods. One of the methods involved using the simple general equation

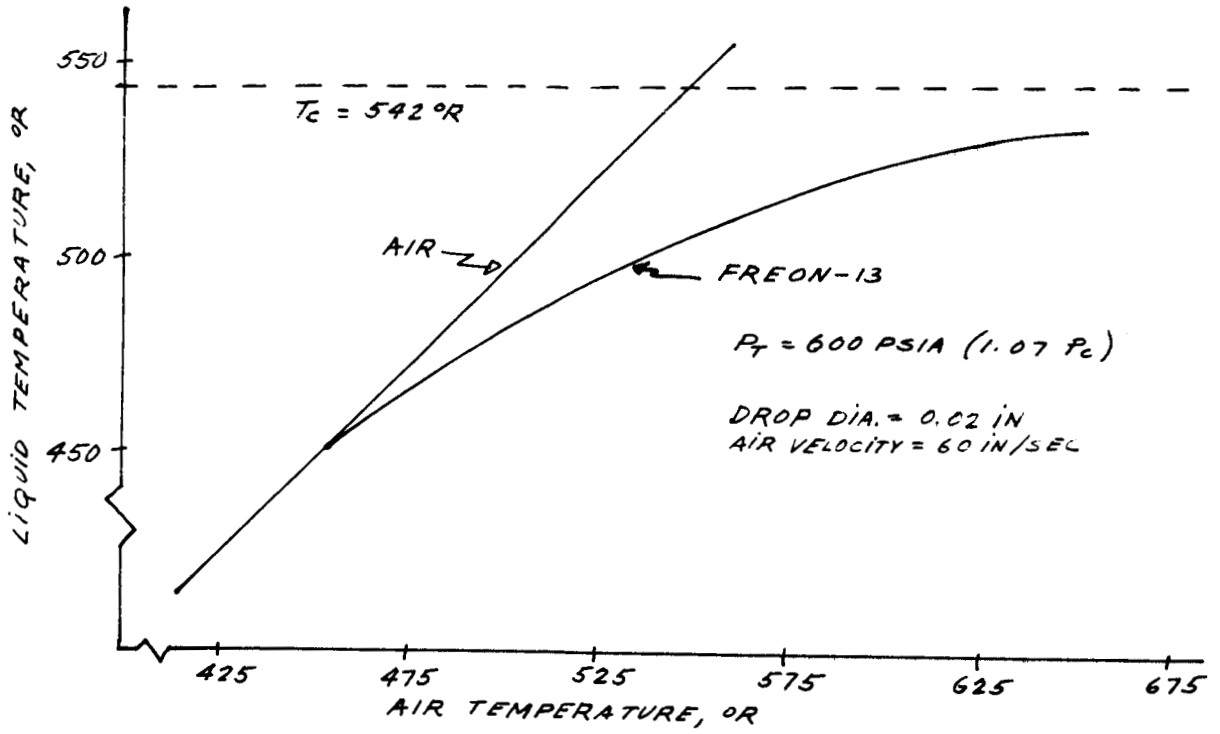

Fig. 9 - Steady State Temperature for Freon-13

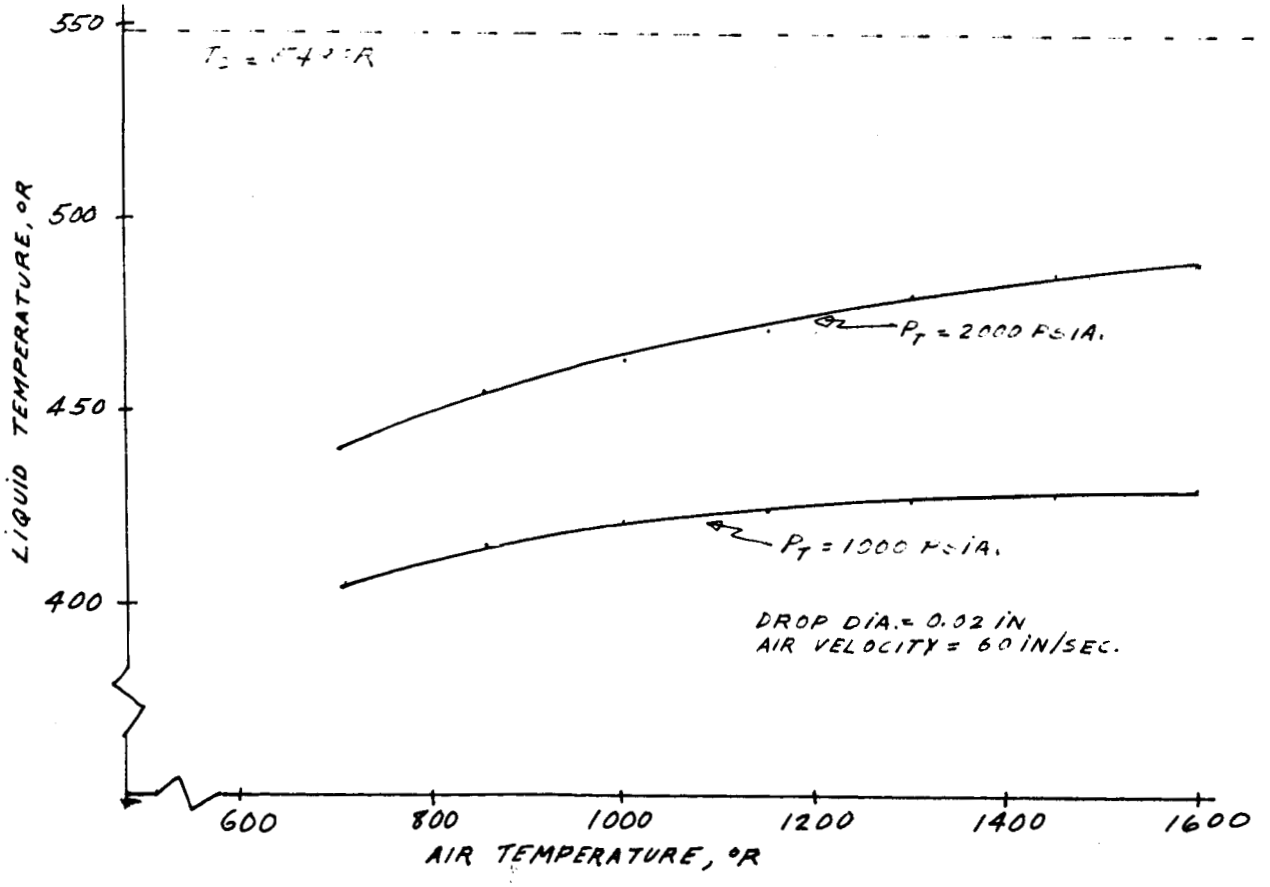

Fig. 10 - Steady State Temperature for Freon-13

that was used in finding the diffusivity coefficient for Freon-13, the other method involved using the Lennard-Jones parameters for n-dodecane. The latter method is the more accurate one of the two. The two coefficients were then compared and it was found that they differed by a factor of nearly eight, with the simpler method yielding the larger coefficient. The next step was to calculate the coefficient of diffusivity for Freon-13 using the simpler method at the same reduced temperature and reduced pressure used in the n-dodecane calculations. This coefficient was then corrected by the factor obtained in the n-dodecane calculations. The last step was to calculate the Schmidt and Nusselt numbers with the corrected diffusivity coefficient. The results obtained by these calculations yielded a Schmidt number approximately equal to one. The ratio of the Nusselt numbers was calculated to be nearly one. The steady state temperature was not calculated after the introduction of the correction factor because the use of such a factor can not be justified scientifically. Additional work on these property calculations in continuing.

Computations for the steady state temperature of ethane were run for total pressures of 1000 psia (1.4 P_c) and 2000 psia (2.8 P_c). Fig. 10 shows thatat 1600 °R and at the higher pressure the liquid temperature is only 487 °R and quite steady with changes in the air temperature. Since this temperature is 61 °F below the critical temperature, ethane is not a good experimental fluid. Possibly the reason for this early flatten-

ing of the liquid temperature curve is the relatively high heat of vaporization of ethane.

The most important part of the apparatus is the high pressure bomb in which the probe is located. The only other necessary equipment is the air heater. If Freon-13 is used, a low temperature air heater is needed. If a hydrocarbon is used, a high temperature air heater, capable of heating the air to about 2300 °R, is needed. Inasmuch as we are now thinking of using a Freon, at least in the preliminary research, it was decided to concentrate our efforts on designing the high pressure bomb and probe. Both the high pressure bomb and probe have been designed to sustain the high temperatures that will be encountered in latter research with hydrocarbons. A layout diagram of the set-up is shown in Fig. 11.

The bomb has to be able to withstand pressures of about 1000 psia and temperatures of about 2400 °R and openings must be available for observing the drop and for insertion of the probe. Fig. 12 shows cross-sections of the bomb. The bomb is now being fabricated from a block of forged SS 124. Since the walls of the bomb are thick, the optics necessary to observe the droplet will be located inside the bomb. It is proposed to mount the optics in a sleeve that will fit closely in the window borings. The optical path can be made as long as necessary, outside of the bomb, to obtain the desired magnification.

The most difficult component to design is the probe and

1 Brass Double Electrode
2 Slotted Teflon Arc Guide
3 Lucite Body
4 Fused Quartz Window
5 Brass Single Electrode

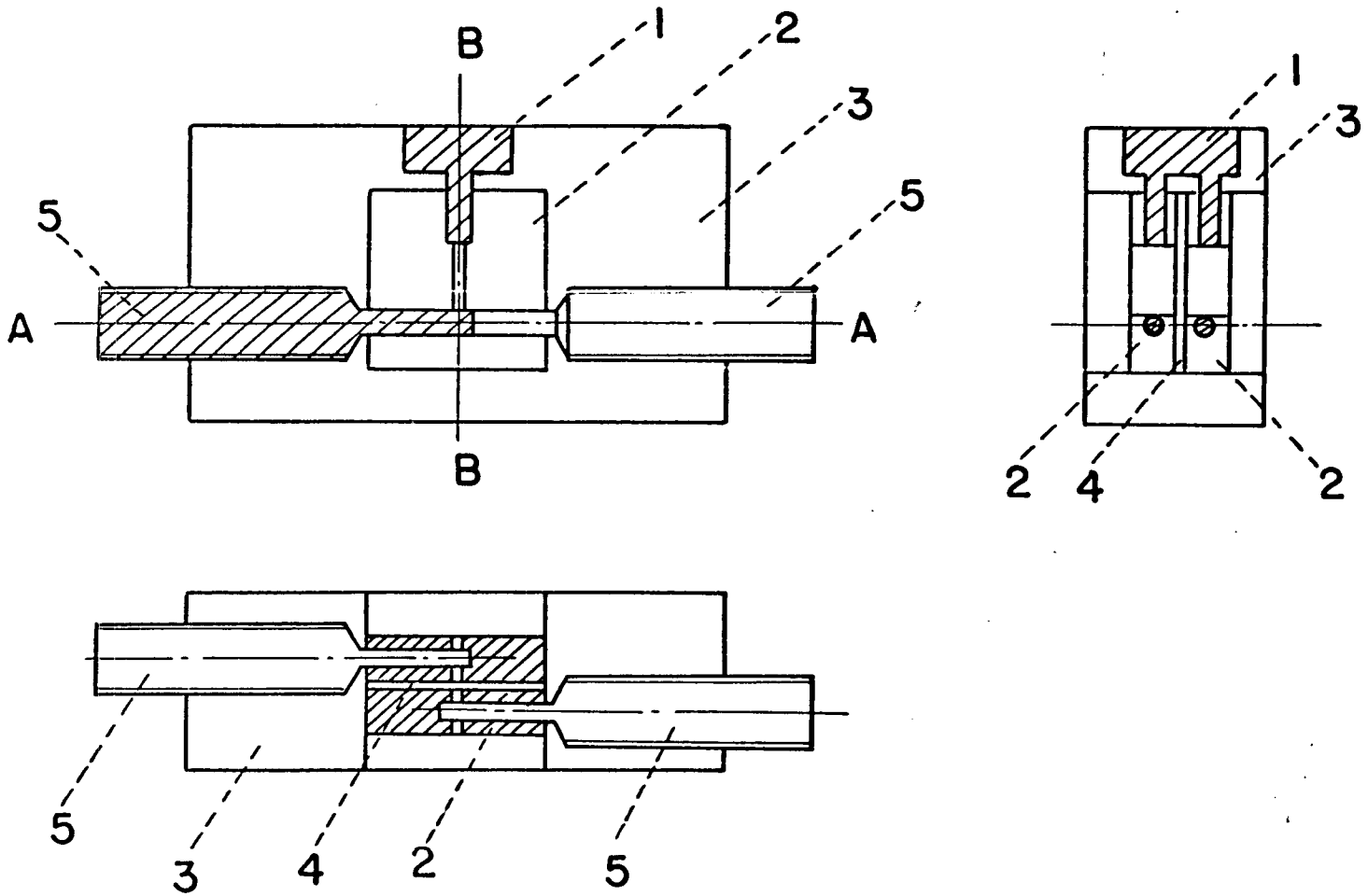

Fig. 11 - Single Location Double Flash Source

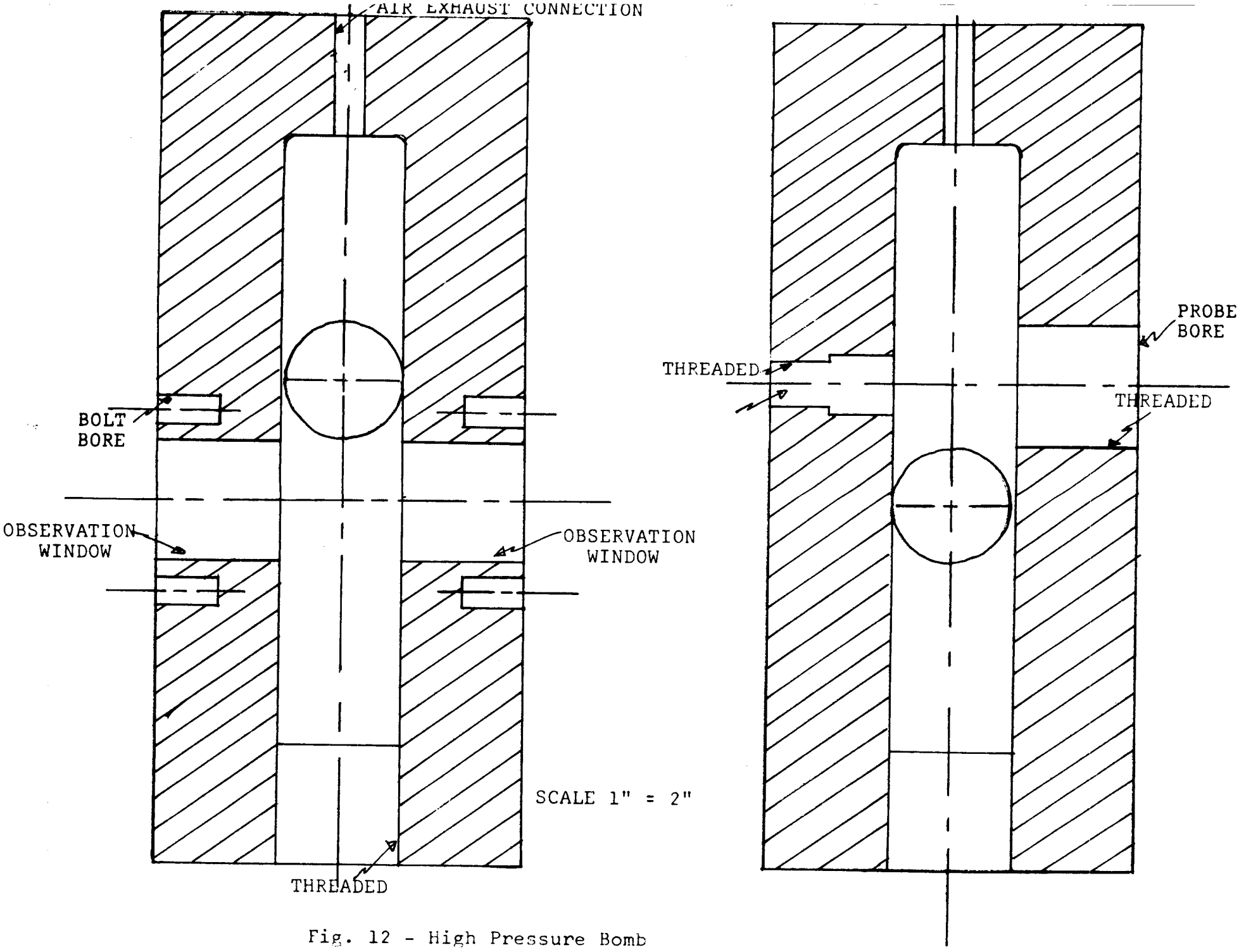

Fig. 12 - High Pressure Bomb

related equipment. The probe itself must be sturdy and, in addition, it must provide for cooling, control and metering of the mass rate of flow, measurement of the initial temperature of the fluid, and measurement of the droplet core temperature. The probe must also be able to accomodate the maximum mass flow rate to be encountered in the experiments without undue pressure loss. The proposed design of the probe, shown in Fig. 13, consists mainly of a quartz tube encased in a stainless steel sheath.

A reservoir outside of the bomb supplies coolant which passes through the walls of the bomb and from there through the stainless steel sheath. If Freon is used, water will be an adequate coolant.

The mass rate of flow necessary to keep the droplet size constant was calculated to be 3.12×10^{-3} lb_m/hr at a liquid temperature of 534 °R. A curve of this mass flow rate versus liquid temperature is shown in Fig. 14. This mass rate of flow is quite small. It must be noted that the accuracy of this value is limited by the accuracy of the property equations as already discussed above. To measure this small flow rate, it is proposed to measure the pressure drop through a cooled capillary. Notice that the capillary shown in the diagram of the probe is straight; this is for the sake of clarity. The mass rate of flow will be controlled by a needle valve. The two thermocouples shown in the diagram measure the droplet core temperature and initial liquid temperature.

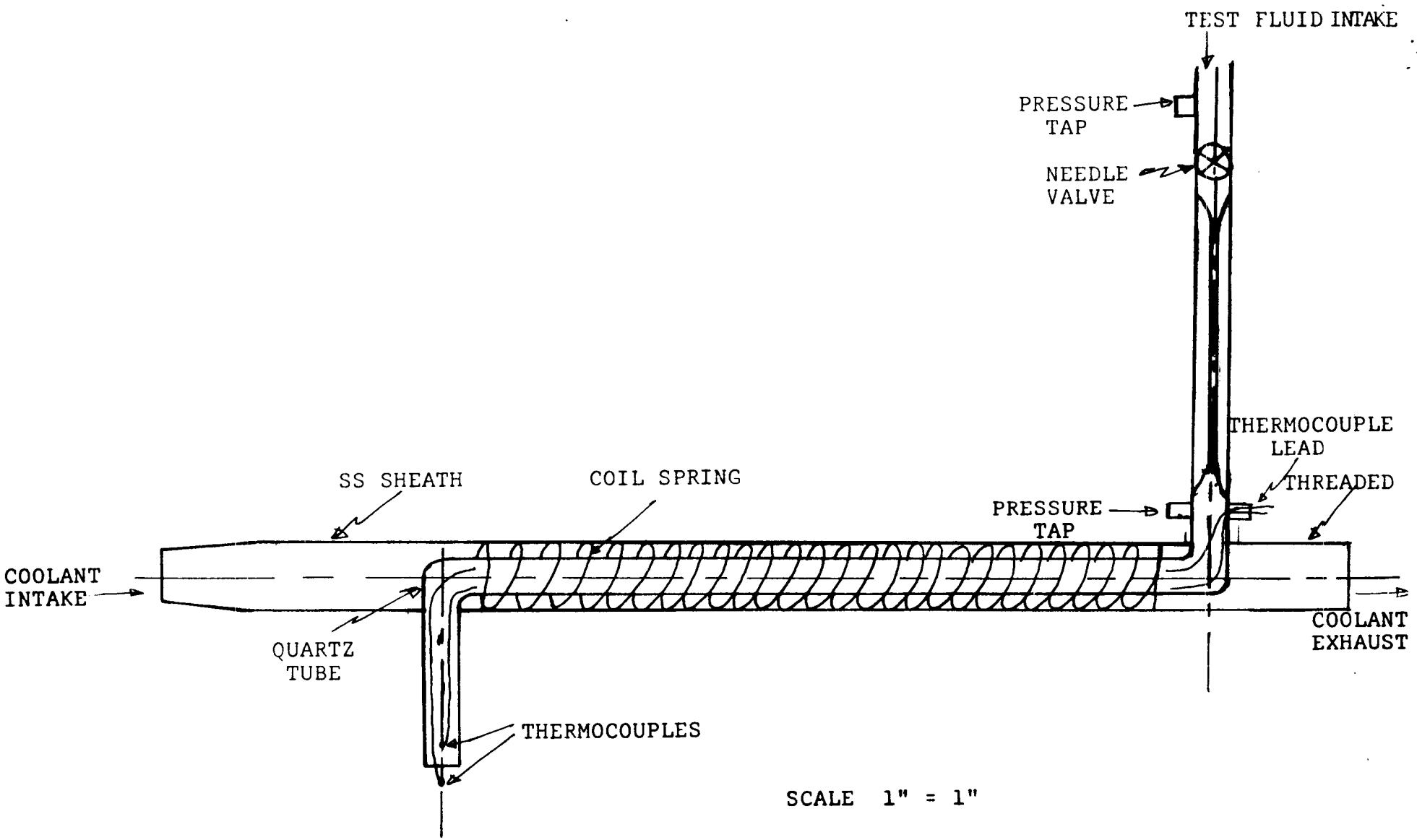

Fig. 13 - Liquid Probe

Fig. 14 - Mass Rate of Evaporization Vs. Temperature for Freon-13

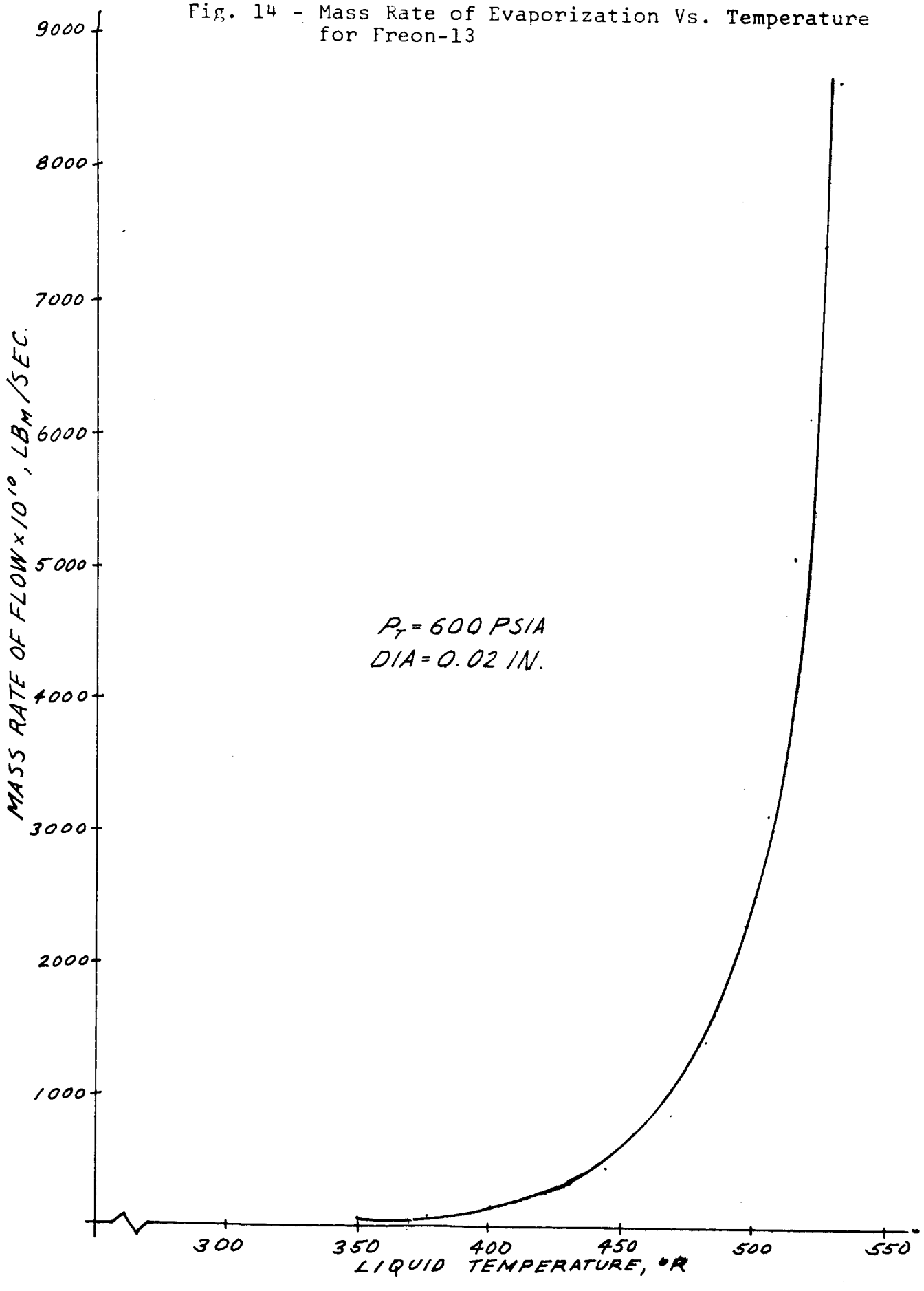

APPENDIX A

Details of the Apparatus for Measuring Drop Sizes and Velocity Distributions in Sprays

High Voltage Power Supply and Capacitors

Fig. 1 is a schematic of the high voltage power supply. It is adjustable in two ranges, 0 - 25 kv and 0 - 50 kv. It charges the two light source capacitors to 35 kv in about 40 seconds so that one timed double exposure can be obtained for each 45 second of running time when everything is operating properly.

The high voltage energy-storage capacitors are not identical but both are low inductance types. The capacitor on the right is a Cornell-Dubilier NRG-341 having a peak operating voltage of 40 kv, a capacitance of 0.1 mfd, and an inductance of 0.010 micro-henries. The capacitor on the left is a unit with similar ratings that was made to order by the Line Material Co. of Milwaukee, Wisconsin.

Light Source Control Switchs and Trigger Generators

The first light source control switches that were tried were three electrode spark gap switches in air at atmospheric pressure. These proved unsuitable for controlling accurately timed discharges at the voltages we were interested in for two main reasons: corona discharges in the main gap made triggering unpredictable and sensitive to atmospheric conditions; the large gap between the main electrodes that was necessary because of the high voltages caused an unpredictable delay between application of the trigger pulse and the

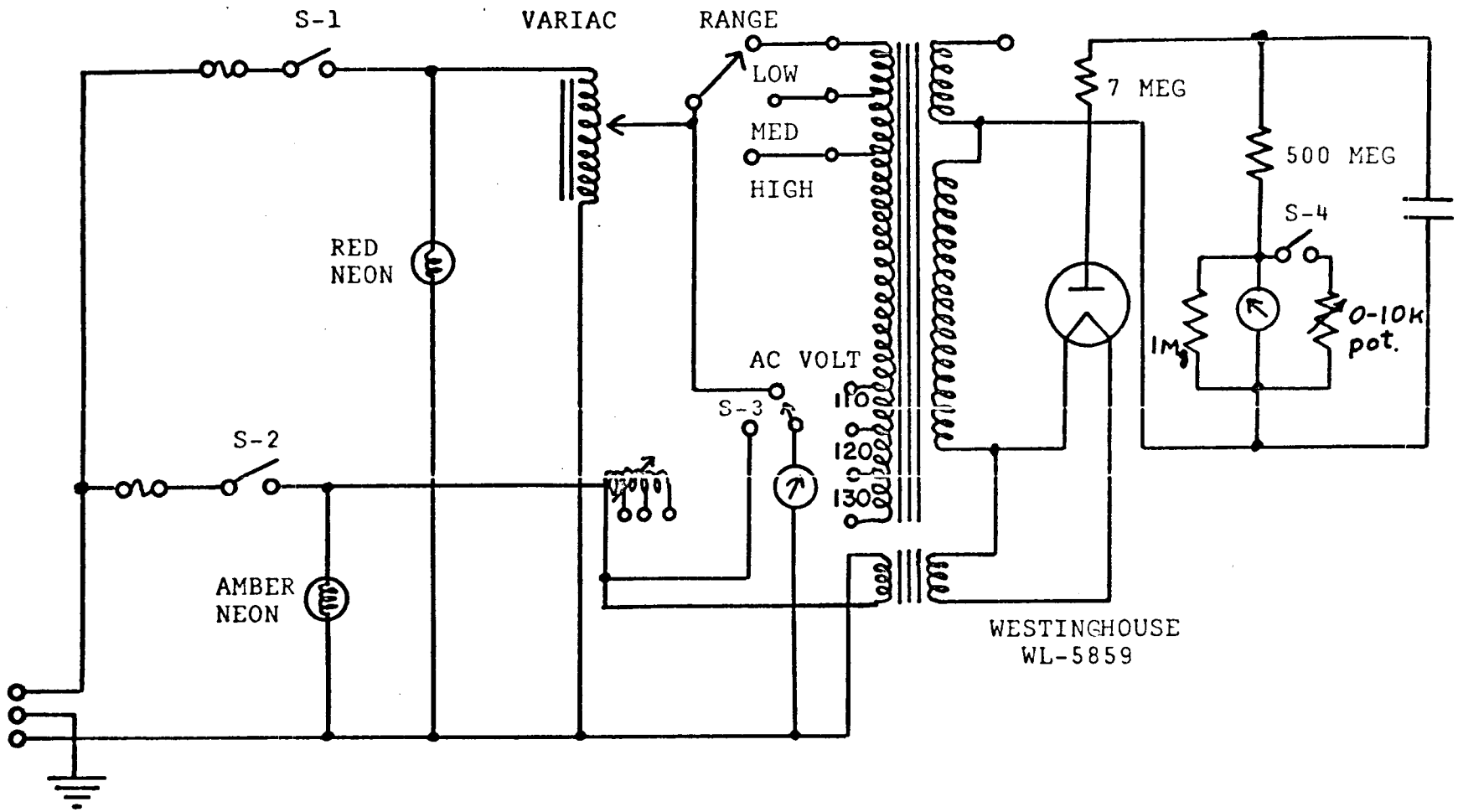

Fig. 1 Schematic of the High Voltage Power Supply

actual firing of the switch. Another shortcoming of these open air switches was that adjusting them for a particular operating voltage required respacing the electrodes until correct operation was achieved. This was time consuming and the setting for a given voltage could change from day to day because of changing atmospheric conditions.

In order to overcome the shortcomings that are mentioned above, a pair of pressurized three electrode spark gap switches were built. These have many advantages over the open air spark gap switches including quick and easy adjustment. By operating at higher than atmospheric pressure, closer electrode spacing is possible. This permits a more suitable ratio of trigger gap length to main gap length which leads to a very much shorter and more predictable delay between the application of the trigger pulse and the breakdown of the switch. Assuming main electrodes of spherical profile, the critical factors in the performance of such switches are: 1) the operating voltage, 2) the main gap length, and 3) the ratio of trigger gap length to main gap length. This style of spark gap switch gives the best results when operated with a trigger wire that goes positive mounted near the positive main electrode.

Fig. 2 is a drawing of the type of spark gap switches that were developed to control the light sources. These switches are pressureized with dry nitrogen from a compressed nitrogen cylinder. The pressure is controlled by means of an ordinary nitrogen pressure regulator. Fig. 3 shows breakdown voltage versus gauge pressure obtained from experiments with

1 Hollow Brass Electrode
2 Trigger Wire
3 Plexiglass Tube
4 Brass Electrode
5 Neoprene O ring Seal
6 Plexiglass Lower Flange
7 Plexiglass Upper Flange
8 Brass Pressurizing Fitting

The upper and lower flanges and clamped together by means of six 6 x 32 screws.

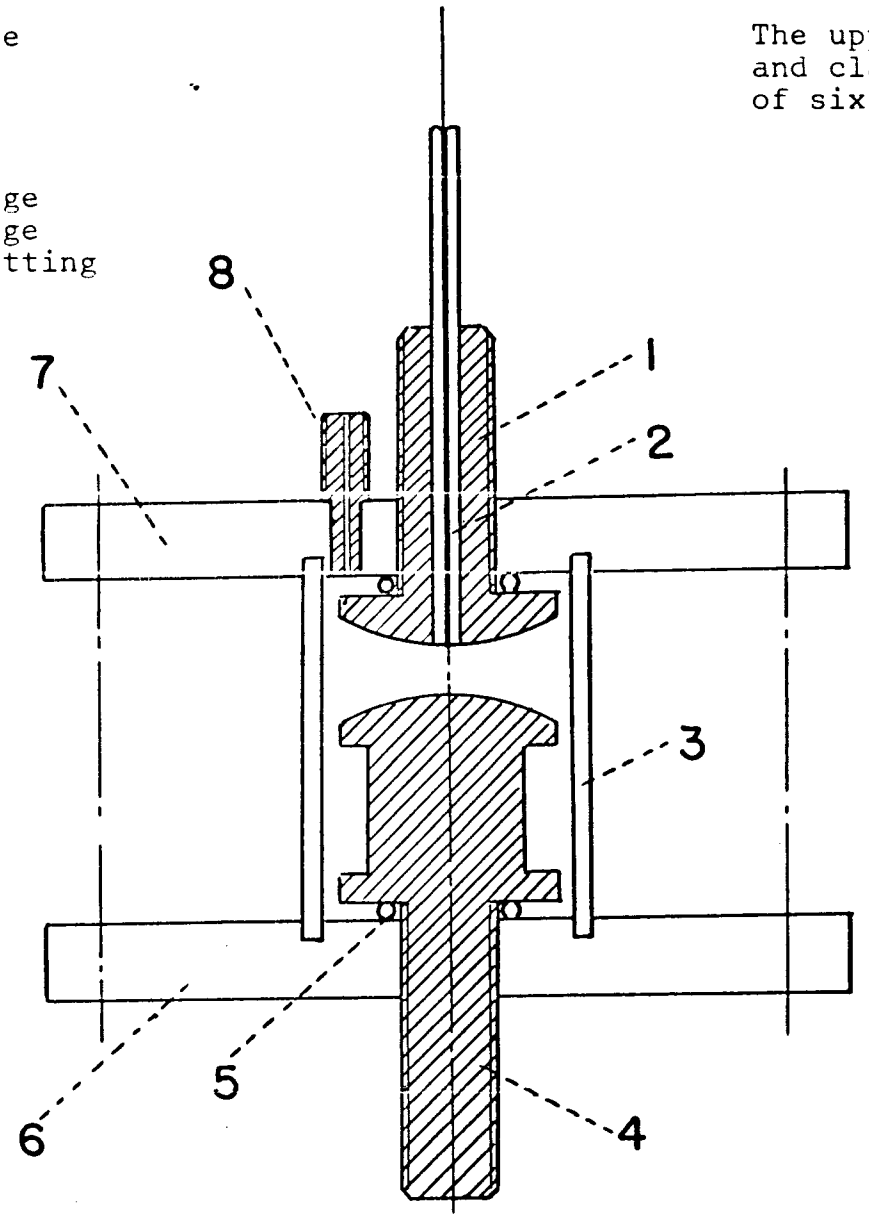

Fig. 2 - Spark Gap Switch

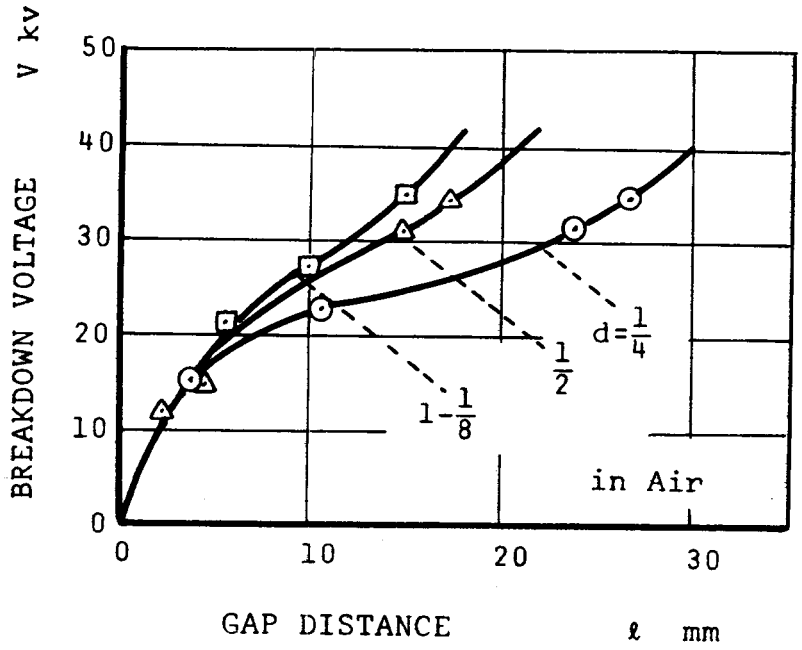

Fig. 3a - Breakdown Voltage at Atmospheric Pressure Versus Electrode Separation and Electrode Diameter

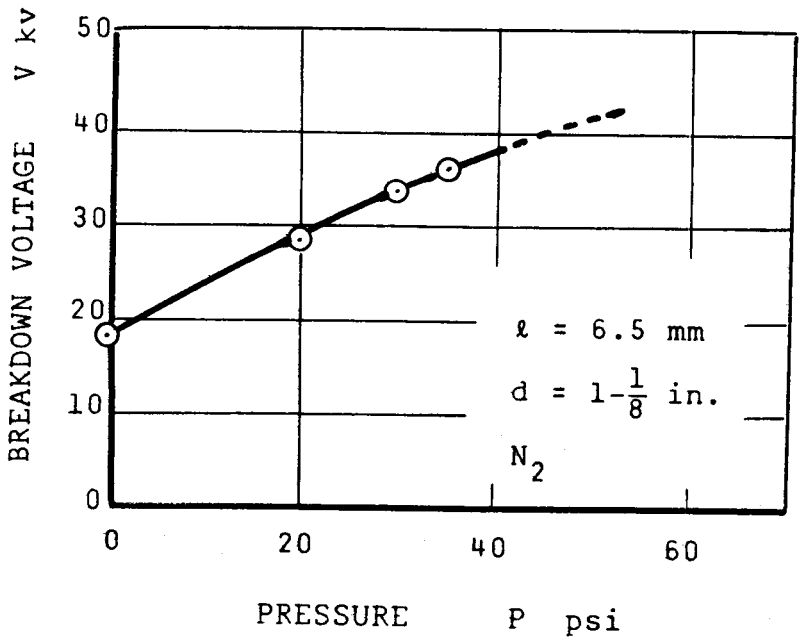

Fig. 3 - Breakdown Voltage Versus Gauge Pressure for Spark Gap Switch with 6.5 mm Electrode Spacing

1/4 in. electrode separation. This curve is useful for selecting the initial pressure when setting the switches to operate at a particular voltage but because of interactions which tend to cause the second switch to fire when the first switch is fired, the final pressure setting of the second switch must be made experimentally. Because different pressures are needed on the two switches, two nitrogen regulators and two nitrogen cylinders are used. Each spark gap switch is fired by its own trigger generator and pulse amplifier combination. Fig. 4 is a schematic of the type of trigger generator that was used with these spark gap switches. These trigger generators will accept either a manual or a +20 volt input and have been very reliable.

Line Light Sources

Fig. 5 shows the design of the constricted arc line light source that was developed from those used previously for drop size pictures. The only part of this light source that wears seriously is the slot in the teflon block that constricts the arc. These teflon blocks are replaced when they wear enough so that the quality of the drop pictures begins to suffer. When the capacitors are charged to 35 kv, the life of the teflon block is from 300 - 400 usable discharges.

Condensing Lenses and Light Axis Arrangement

The condensing lenses are used to collect some of the light from the line sources and form it into a sheet of light in the

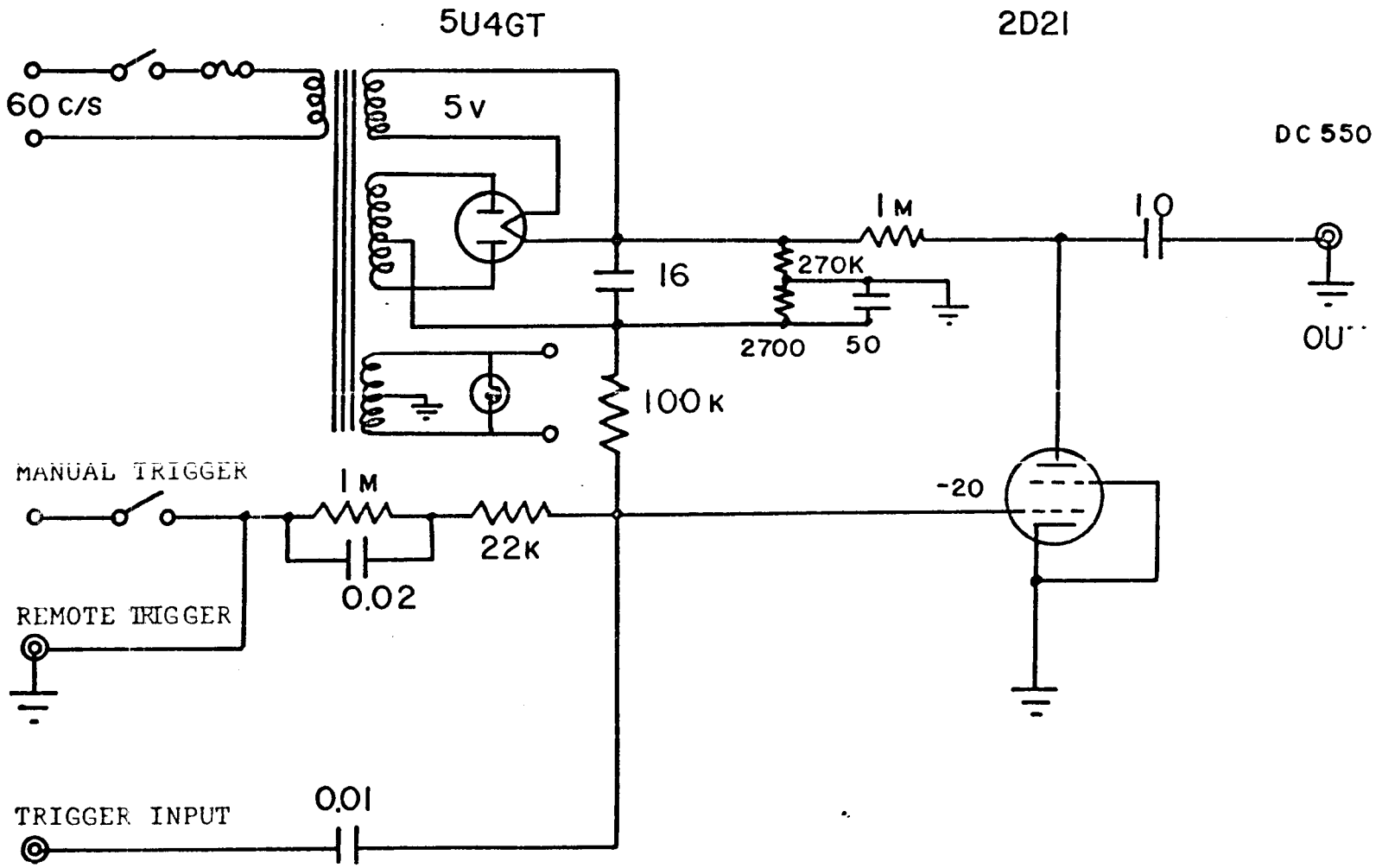

Fig. 4 - Schematic of Trigger Generator

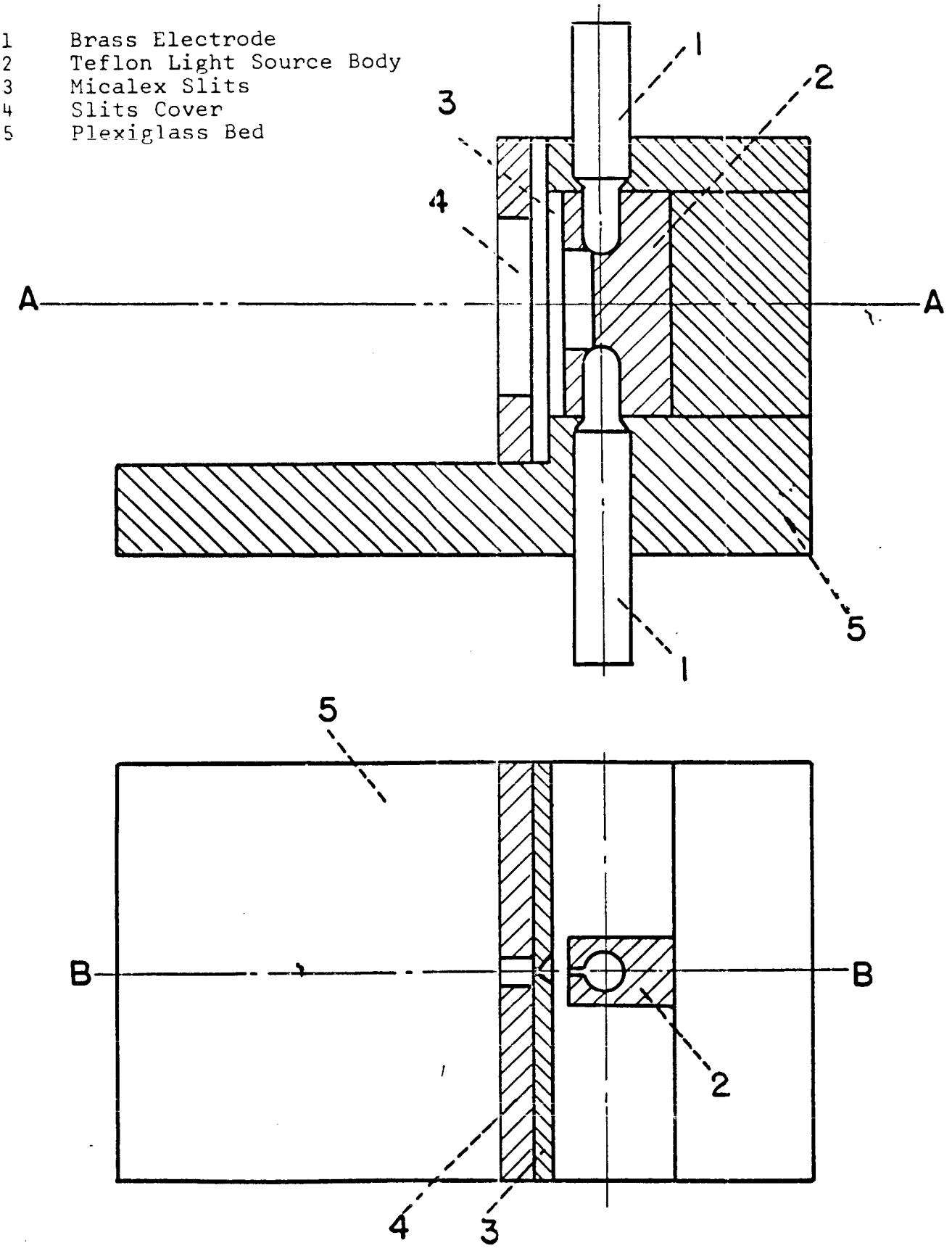

Fig. 5 - Line Light Source

object space of the camera. Because they must transmit ultraviolet light, they are made of fused quartz. As they are now used, the condensing lenses form a light sheet that is about 1/4 the height and thickness of the line source aperture. The condensing lenses on the right are part of the original equipment while those on the left were obtained during the last year. They are similar to but not exactly the same as those on the right. The new condensing lenses are mounted in a holder that is capable of easy adjustment in three dimensions plus a small degree of rotation. The light source holder on the left is capable of the same adjustments as the condensing lens.

Photographic System

The camera is the same one that was developed in the past for measuring drop size distributions. It was developed early in this project and is very suitable for photographing drops from 10 microns in diameter up. It is now set up with a 25 times linear magnification but this is adjustable to a certain extent. It uses a sheet film camera back and a two lens system without a shutter. It is operated in a darkened room because there is no shutter and this prevents stray light from fogging the film.

The droplet pictures are taken on 4 in. by 5 in. Royal X Pan sheet film. The film is processed in Kodak DK - 60a developer at 68 °F for 12 minutes, then fixed and washed

normally. Following this, it is intensified using Monckhoven's Intensifier, then washed and dried normally.

Flash Duration Monitoring and Flash Delay Control

Samples of the light output from both light sources are directed by mirrors to the same photo tube as shown in Fig. 6, which is a modified block diagram of the firing control and monitoring circuitry. The duration, relative intensity, and timing of the light pulses are observed on an oscilloscope. The oscilloscope has an adjustable delayed trigger output that operates from one of its time bases. The first light pulse is initiated by manually firing the first trigger generator. Then the signal from the photo tube circuit starts the scope trace and thus starts the delay period. After a preset delay period, the output trigger pulse supplied by the scope is fed to a pulse amplifier. The output of the pulse amplifier fires the second trigger generator which in turn fires the switch of the second light source. Schematic diagrams of the photo tube circuit and the pulse amplifier circuit are given in Fig. 7 and Fig. 8 respectively.

Spray Control System and Liquid-Fluorescent Dye Mixture

Fig. 9 illustrates the apparatus that causes, controls, and measures the flow of the fluid that is being investigated. The liquid mass flow rate is adjusted by adjusting a nitrogen pressure regulator and measured by means of a platform scale

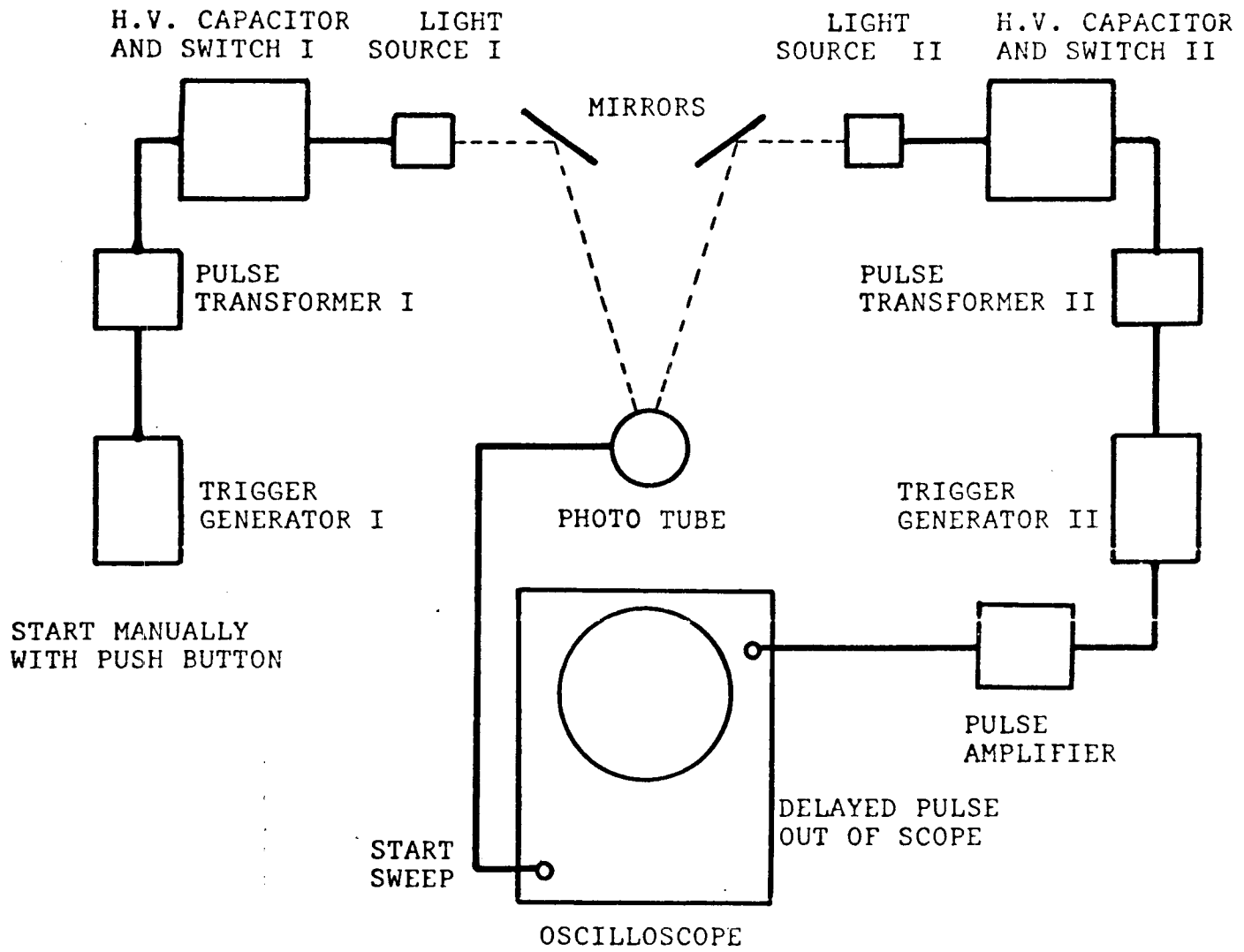

Fig. 6 - Block Diagram of the Firing Control and Monitoring Circuitry

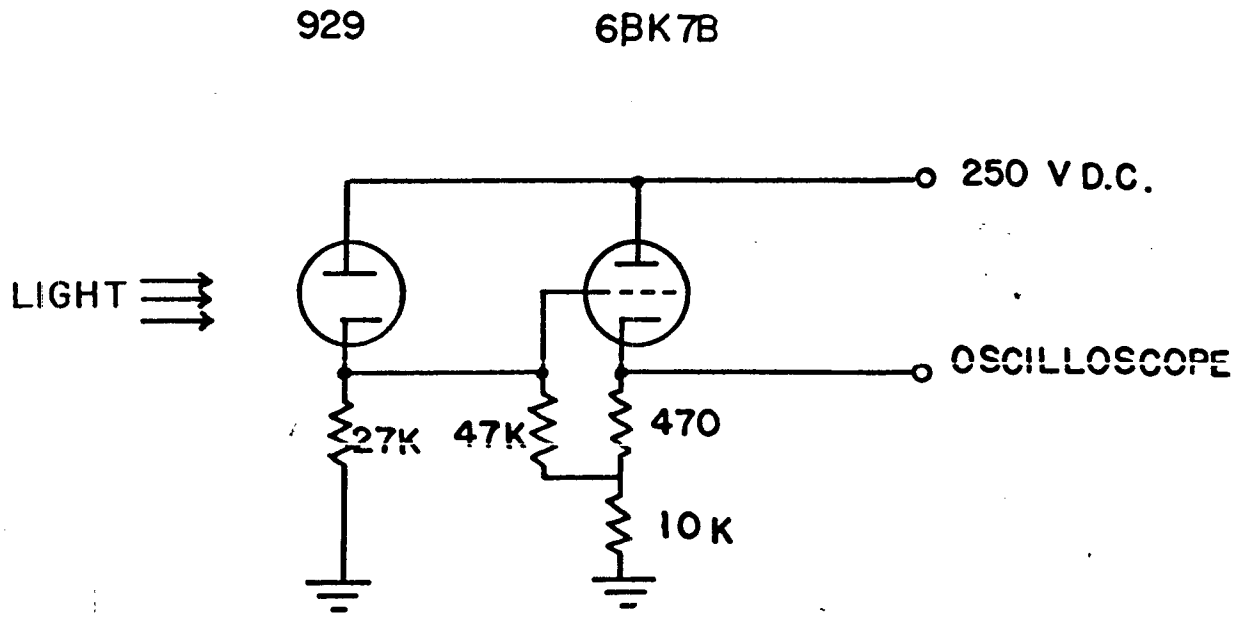

Fig. 7 - Diagram of the Phototube Circuit

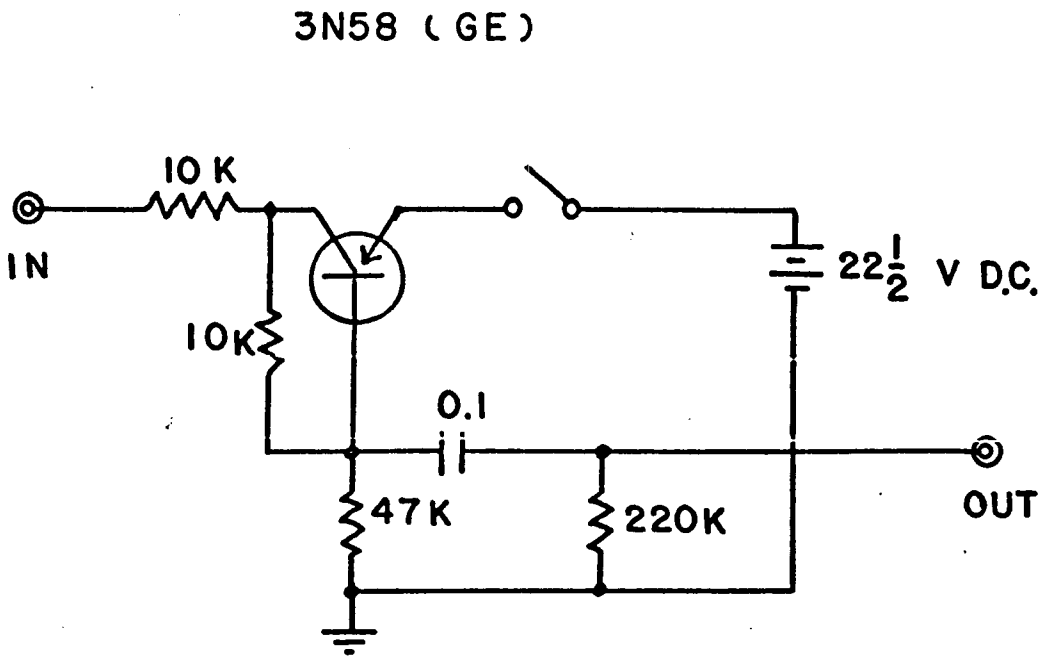

Fig. 8 - Diagram of the Pulse Amplifier Circuit

1 Nitrogen Bottle
2 Nitrogen Bottle Valve
3 Pressure Gauge
4 Pressure Regulator
5 Filling Funnel
6 Filling Valve
7 Spray Fluid Pressure Tank
8 Valve
9 Platform Scale
10 Nozzle Pressure Drop Gauge
11 Nozzle
12 Exhaust Duct
13 Exhaust Fan

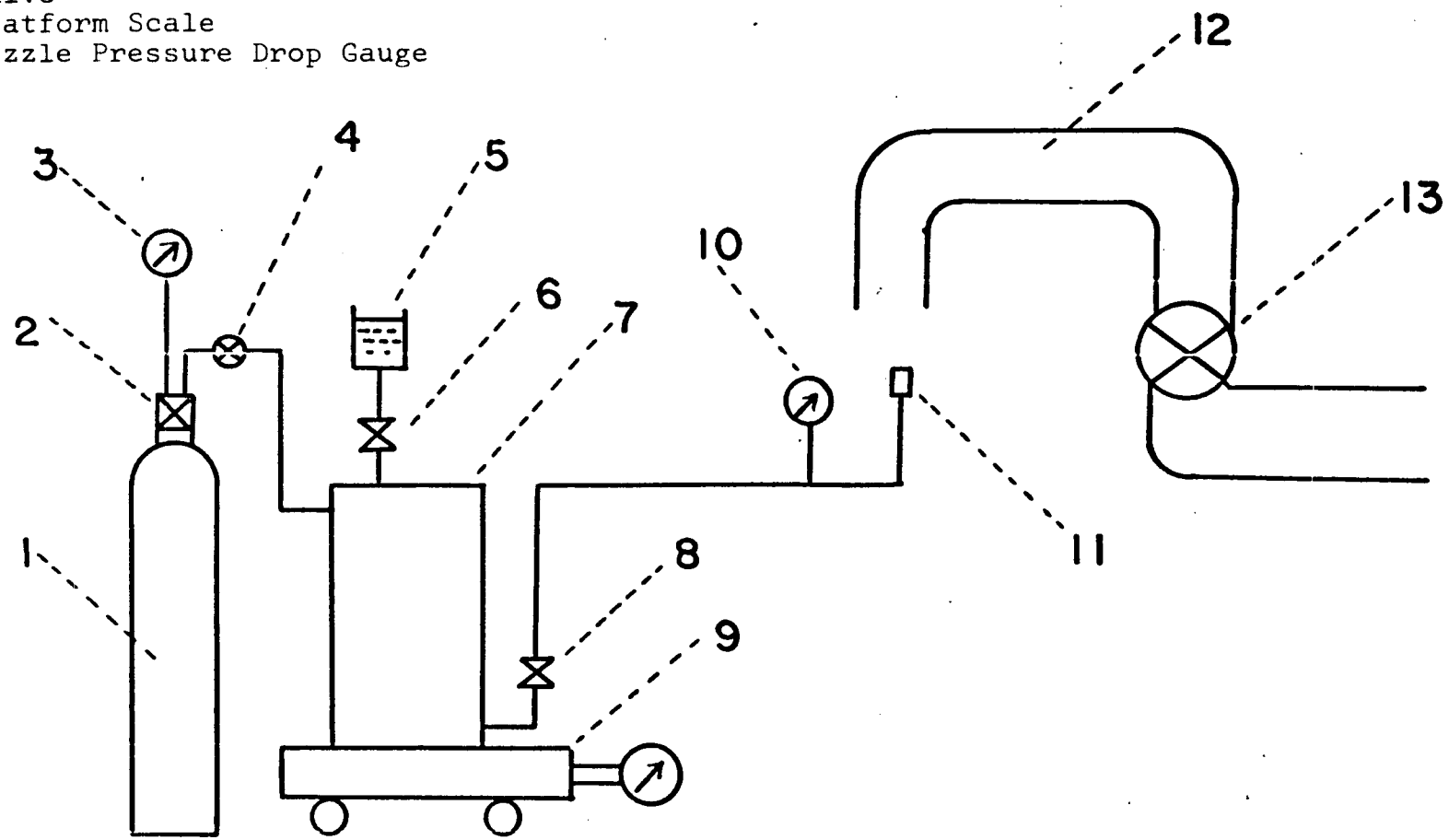

Fig. 9 - Schematic of the Fluid Flow Control Apparatus

and a lab timer. The spray liquid, the vapor, and the entraining air are carried outside by an exhaust fan in the air duct.

The velocity data taken with the apparatus so far have used ethyl alcohol as the spray fluid. The ethyl alcohol that is used is the 95% grade in which is dissolved 5 grams per liter of Fluorescein water soluble Uranin (WSS Tech) dye.

Some Unsuccessful Methods

The initial attempts to devise a suitable double flash light source made use of two energy storage capacitors and a single line light source. Fig. 10a and Fig. 10b illustrate two of several circuits that were tried. These circuits are similar to those used successfully for taking shadow pictures by H.E. Edgerton and others at much lower voltages and smaller energies. The arrangement of these circuits was dictated by the facts that the power supply gives a negative high voltage, the capacitor cases are connected internally to one of the plates, three electrode spark gap switches operate best with a positive going trigger electrode mounted near the positive main electrode, and the trigger generator and pulse transformer combination give a positive trigger pulse.

Both the above circuits worked satisfactorily for delays between light pulses of greater than 100 microseconds. As the delay between light pulses is reduced from 100 microseconds, the second light pulse is of progressively weaker intensity, at least for the wavelengths of interest in the fluorescent technique. Finally, for delays of less than 35 - 40 microseconds,

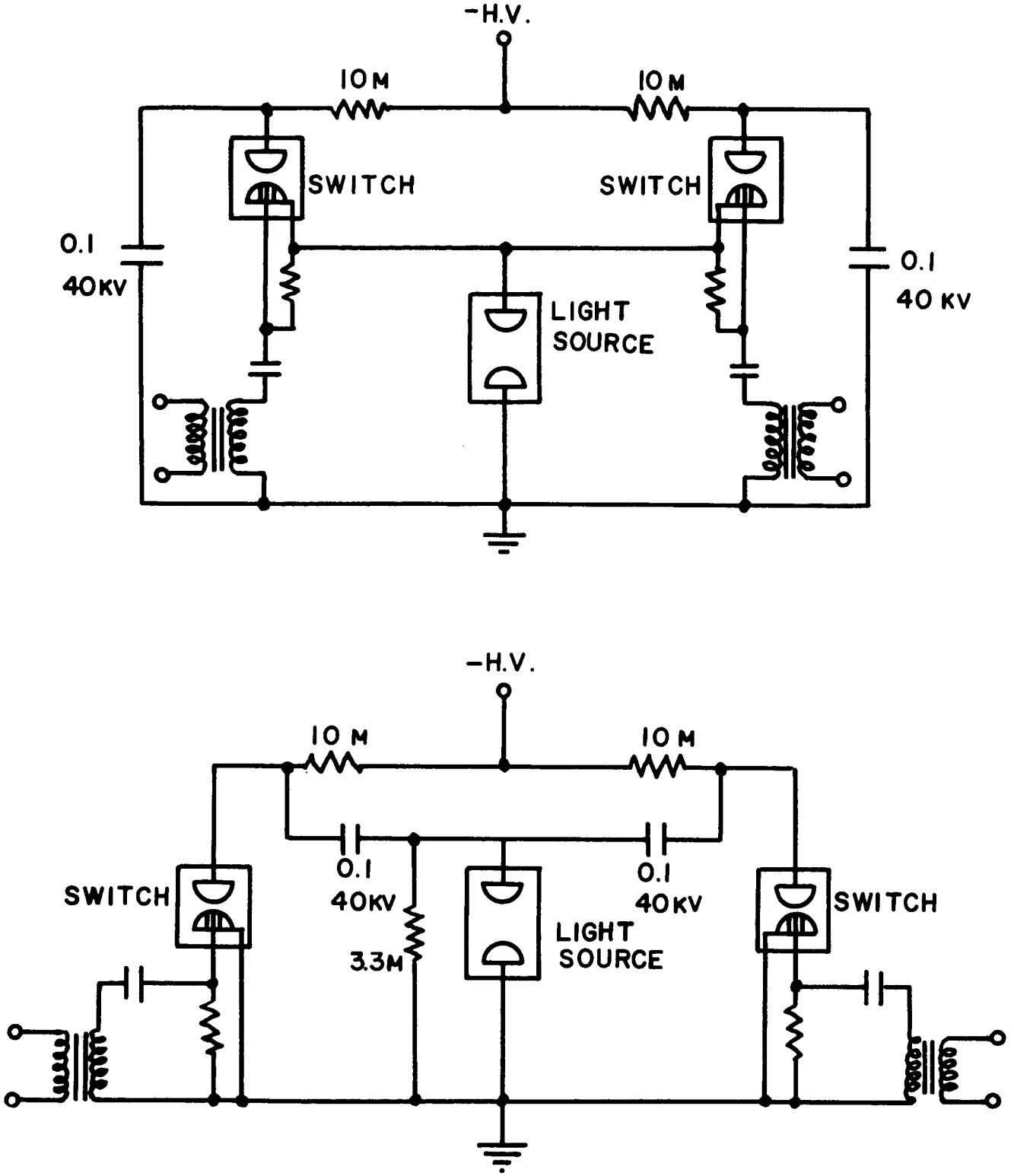

Fig. 10 - Two Unsuccessful Double Flash Light Source Circuits

the second light pulse becomes too weak to produce any images on the film. The reason for this behavior is not completely understood, but seems to be related to the deionization time of the gas in the light source and first switch gaps. If the second switch is fired before the first switch has recovered sufficiently, a large part of the energy that sould be going to the light source gap may be dissipated in the gap of the first switch. Another possible explanation for the weak second light pulse is that the radiation caused by the second current pulse occurs at wavelengths that do not strongly affect the film, the fluorescent dye, or the photo tube and perhaps are not transmitted well by the optical system.

Fig. 11 illustrates one method that was tried to construct a light source that acted as much as possible like a single line source optically, while acting like two separate line sources electrically. Essentially, one line source was placed behind the other with a thin insulating window between. First a window of 1/16 in. plexiglass was tried. With it, some double flash pictures were taken with any desired delay between the light pulses. The light pulses from the light source behind the window, however, were very weak and produced images on the film that were too faint to take measurements from. Fused quartz windows 1/16 in. thick were tried in order to cut down the light losses due to the window. The result was one broken fused quartz window for each pair of discharges. Since replacing the fused quartz window was time consuming and difficult, no serious attempt was made to see if a one fused quartz

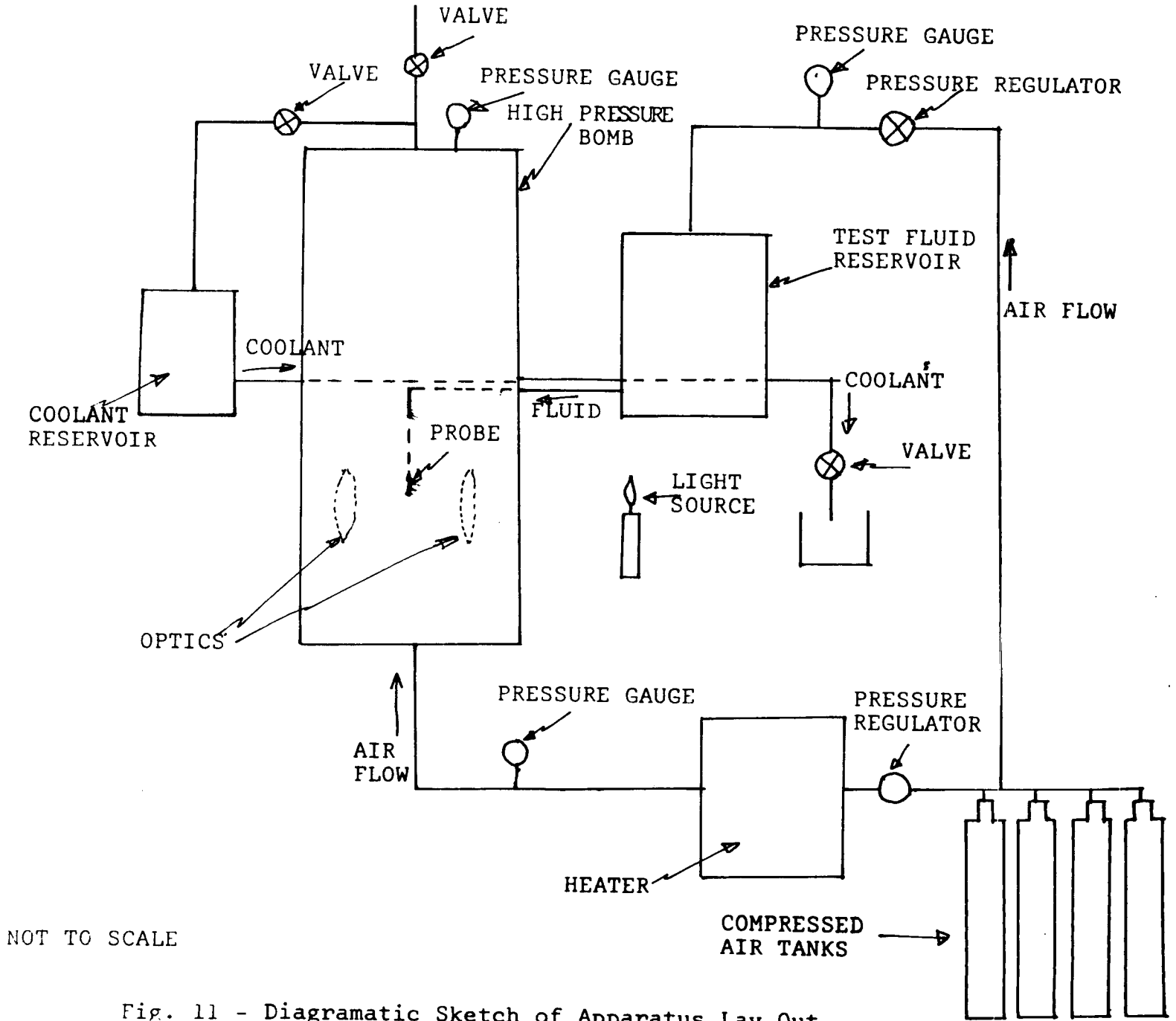

Fig. 11 - Diagramatic Sketch of Apparatus Lay Out

window for one timed-double-exposure picture could be made.

The possibility of using some kind of beam splitter to cause two line light sources to act optically as a single line light source was investigated. This again would have the advantage of requiring only one condensing lens and could use the spherical mirror to light the side of the drop away from the light source. Fig. 12 illustrates the basic idea. The usual variety of beam splitting mirror that might be used in this way loses considerably more than half the light because of surface reflection and internal absorption losses for the transmitted beam and the losses from incomplete reflection of the reflected beam. One possible way of overcoming some of these objections is to use a beam splitter made of narrow strips of high quality first surface mirror with equal open spaces between. Some simple tests were performed by blocking half the aperture of the condensing lens with strips of black paper of various widths. These tests indicated that this technique could be used with the previously described line sources to take usable pictures that would yield drop velocity. The optical companies that were contacted showed no interest in making such a mirror so the idea was put aside without further tests.

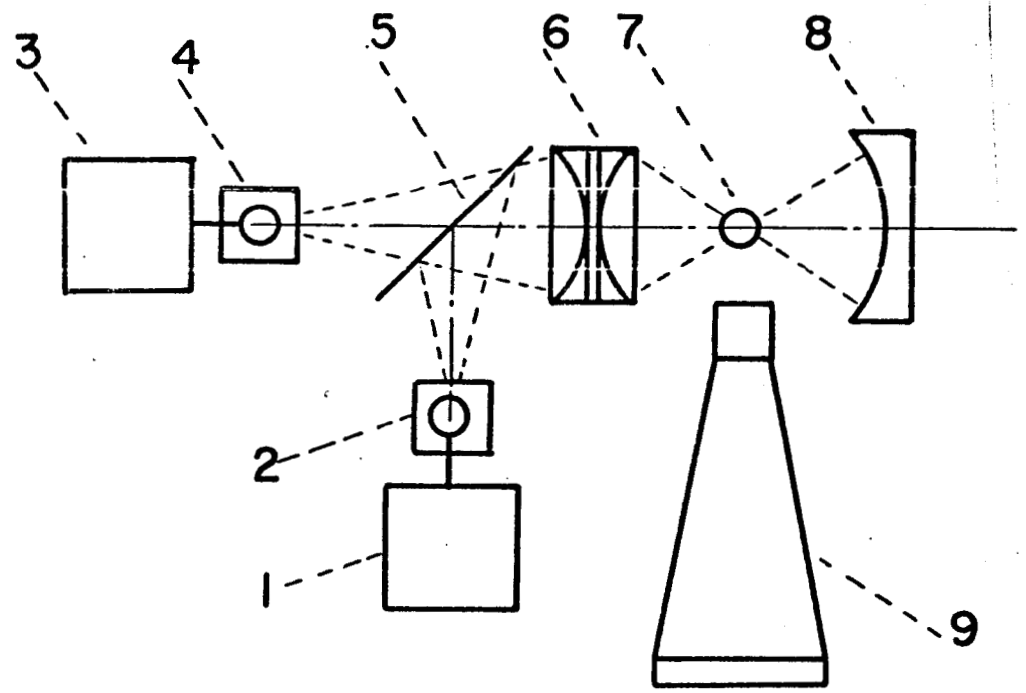

Fig. 12 - Double Flash Apparatus Using Two Light Sources and A Beam Splitter